

**Earth Surface
Processes and Landforms**

**The influence of structural organization of epilithic and
endolithic lichens on limestone weathering**

Journal:	<i>Earth Surface Processes and Landforms</i>
Manuscript ID	ESP-16-0312.R1
Wiley - Manuscript type:	Research Article
Date Submitted by the Author:	10-Jan-2017
Complete List of Authors:	Morando, Mariagrazia; University of Torino, Life Sciences and Systems Biology Wilhelm, Katrin; University of Oxford, School of Geography and the Environment Matteucci, Enrica; University of Torino, Life Sciences and Systems Biology Martire, Luca; University of Torino, Earth Sciences Piervittori, Rosanna; University of Torino, Life Sciences and Systems Biology Viles, Heather; University of Oxford, School of Geography and the Environment; Favero-Longo, Sergio; University of Torino, Life Sciences and Systems Biology
Keywords:	biodeterioration, lichen-rock interface, stone cultural heritage, surface hardness, water absorption capacity

SCHOLARONE™
Manuscripts

The influence of structural organization of epilithic and endolithic lichens on limestone weathering

Morando M.¹, Wilhelm K.², Matteucci E.¹, Martire L.³, Piervittori R.¹, Viles H.A.², Favero-Longo S.E.^{1,*}

1 - University of Torino, Department of Life Sciences and Systems Biology, Viale Mattioli 25, 10125, Torino, Italy

2 - Oxford Rock Breakdown Laboratory (OxRBL), School of Geography and the Environment, University of Oxford, Oxford, UK

3 - University of Torino, Department of Earth Sciences, Via Valperga Caluso 35, 10125, Torino, Italy

*Corresponding author:
Sergio Enrico Favero-Longo
University of Torino, Department of Life Sciences and Systems Biology
Viale Mattioli 25, 10125, Torino, Italy
Tel. +39-011-6705972 // Fax +39-011-6705962
sergio.favero@unito.it

Abstract

Hyphal penetration, mineral dissolution and neoformation at the lichen-rock interface have been widely characterized by microscopic and spectroscopic studies, and considered as proxies of lichen deterioration of stone substrates. However, these phenomena have not been clearly related to experimental data on physical properties related to stone durability, and the physical consequences of lichen removal from stone surfaces have been also overlooked. In this study, we combine microscopic and spectroscopic characterization of the structural organization of epi- and endolithic lichens (*Caloplaca marina* (Wedd.) Du Rietz, *Caloplaca ochracea* (Schaer.) Flagey, *Bagliettoa baldensis* (A.Massal.) Vězda, *Porina linearis* (Leight.) Zahlbr., *Verrucaria nigrescens* Pers.) at the interface with limestones of interest for Cultural Heritage (Portland Limestone, Botticino Limestone), with analysis of rock properties (water absorption, surface hardness) relevant for durability, before and after the removal or scraping of lichen thalli. Observations using reflected-light and electron microscopy, and Raman analyses, showed lichen-limestone stratified interfaces, differing in the presence/absence and depth of lichen anatomical layers (lithocortex, photobiont layer, pervasive and sparse hyphal penetration component) depending on species and lithology. Specific structural organizations of lichen-rock interface were found to be associated with differential patterns of water absorption increase, evaluated by Karsten tube, in comparison with surfaces with microbial biofilms only, even more pronounced after the removal or scraping of the upper structural layers. Equotip measurements on surfaces bearing intact thalli showed lower hardness in comparison with control surfaces. By contrast, after the removal or scraping procedures, Equotip values were similar or higher than those of controls, suggesting that the increasing open porosity may be related to a biogenic hardening process. Such counterposed patterns of porosity increase and hardening need to be considered when models relating

1
2
3
4
5
6
7
8
9
10
11
12
13
14
15
16
17
18
19
20
21
22
23
24
25
26
27
28
29
30
31
32
33
34
35
36
37
38
39
40
41
42
43
44
45
46
47
48
49
50
51
52
53
54
55
56
57
58
59
60

lichen occurrence on limestones and biogeomorphological surface evolution are proposed, and to evaluate the consequences of lichen removal from stone-built cultural heritage.

Keywords

biodeterioration, lichen-rock interface, stone cultural heritage, surface hardness, water absorption capacity

Running head

Impact of lichens on limestone physical properties

For Peer Review

Introduction:

Lithobiontic microorganisms are involved in multiple processes affecting rock surfaces at the atmosphere-lithosphere boundary and the analogous surfaces of stones in buildings and structures (Gorbushina and Broughton, 2009). Microbial influence on geomorphic processes is increasingly considered at all scales of landscape dynamics (e.g. Viles 2012; McIlroy de la Rosa, 2016). Colonization of modern and historic stonework is investigated for its implication for heritage conservation, with potential effects ranging from biodeterioration to bioprotection (Carter and Viles, 2005; Scheerer *et al.*, 2009; Kip and Van Veen, 2015; Tiano, 2016).

A weathering role of lichens, as pioneer colonizers of natural rock surfaces, has been long recognized (Jones, 1988). Lichen deterioration of stone in cultural heritage has also been widely characterized (reviewed, e.g., by St. Clair and Seaward, 2004; Gazzano *et al.*, 2009; Seaward, 2015), although evidence of protective effects has been also unveiled (e.g. McIlroy de la Rosa *et al.*, 2012, 2014, with references therein). Biogeophysical and biogeochemical processes at the rock surface have been ascribed to the attachment and penetration of epilithic and endolithic lichens, and their release of primary and secondary metabolites with acidic and chelating functions, respectively (Adamo and Violante, 2000; Chen *et al.*, 2000; Favero-Longo *et al.*, 2011; Salvadori and Casanova-Municchia, 2016). Advances in microscopic techniques have progressively supported a deeper characterization of lichen structures and associated microbes at the rock interface and their spatial interactions with microstructural features of the substrate and its mineral constituents (de los Ríos and Ascaso, 2005; Favero-Longo *et al.*, 2005; McIlroy de la Rosa *et al.*, 2012; Casanova-Municchia *et al.*, 2014; Mihajlovski *et al.*, 2015). Advanced spectroscopies have allowed the localization and characterization of chemical changes in minerals affected by lichen metabolites (Wierzchos and Ascaso, 1994; Barker and Banfield, 1996) and the detection at the interface of secondary minerals, including clays

and biomineralization products (Wierzchos and Ascaso, 1998; Edwards *et al.*, 2003; Villar *et al.*, 2004). However, such phenomena, considered as proxies to ascertain and quantify rock weathering, have rarely been experimentally related to the durability of stone surfaces and their physical properties.

The influence of lichens on the hardness of rock surfaces has been evaluated for silicate lithologies colonized by epilithic and chasmoendolithic species (i.e. inhabiting cracks and fissures; sensu Golubic *et al.*, 1981) across different climatic areas (McCarroll and Viles, 1995; Matthews and Owen, 2008; Guglielmin *et al.*, 2012; Favero-Longo *et al.*, 2015), but poorly explored for calcareous rocks. Some lichen species have been shown to variously affect the thermal response and moisture retention of limestones, potentially influencing their susceptibility to breakdown (Carter and Viles, 2003, 2004). A waterproofing influence of lichen colonization on the capillary coefficient of oolitic limestones has also been described (Concha-Lozano *et al.*, 2012). However, these studies only partially characterized the lichen component and its physico-chemical interaction with the substrate.

This study combines the characterization of lichen physico-chemical interactions with limestones of cultural heritage interest with the analysis of surface properties relevant for stone durability and weathering. We aimed to verify if the presence of lichens, before and after their removal from the rock surface, may influence/modify the hardness and water absorption characteristics of Portland and Botticino limestones in comparison with exposed surfaces colonized by microbial biofilms only (which are used in this study to represent surfaces exposed to abiotic and biotic weathering, but not colonized by lichens), or freshly broken surfaces (which are used in this study to represent unweathered surfaces). In particular, we aimed to examine if the specific structural organization of some epilithic and euendolithic (i.e. actively penetrating; sensu Golubic *et al.*, 1981) lichens at the rock interface may be related to different effects on limestone physical properties and

potential weathering dynamics in natural environments and on stone-built cultural heritage. The structural organization of the lichen-rock interface was microscopically (reflected light and scanning electron microscopy) and spectroscopically (Raman) characterized, examining the hyphal penetration component (sensu Favero-Longo *et al.*, 2005) for epilithic species and the lithocortex, photobiont and pseudomedulla (sensu Pinna *et al.*, 1998) layers for endolithic species. Surface hardness and absorption capacity/infiltration rates were quantified by Equotip and Karsten tube, respectively.

Materials and methods

Lithologies and lichens

Two limestones largely employed in historical and modern building were sampled in abandoned quarry areas in the Isle of Portland in Dorset (SW-England; WGS-84: N 50°32.334' - W 2°25.548') and Botticino (N-Italy; WGS-84: N 45°32.965' - E 10°18.946'). The samples of Portland Limestone (P), collected in a maritime environment, were representative of a pure-calcite oolitic limestone (Brunsden *et al.*, 1996; Dubelaar *et al.*, 2003). Those of Botticino Limestone (B), deriving from a prealpine area, were micritic, low-magnesium calcite limestones (Borghi *et al.*, 2015). For each lithology, blocks (l × w × h: 15-30 × 15-20 × 15-20 cm) colonized by (a) microbial biofilms (as controls exposed to abiotic and biotic weathering, but not colonized by lichens), (b) epilithic and (c) endolithic lichens were selected for investigations (Figure 1). Biofilms on P and B were composed of filamentous and coccoid green algae, with subordinate cyanobacteria (P-a), and microcolonial fungi and coccoid cyanobacteria (B-a), respectively. Epilithic crustose lichens included *Caloplaca* species with a discontinuous thallus [*Caloplaca marina* (Wedd.) Du Rietz on P: P-bC; *Caloplaca ochracea* (Schaer.) Flagey on B: B-bC], and, on B only, *Verrucaria nigrescens* Pers. (B-bV) with a continuous thallus. Endolithic lichens included *Bagliettoa baldensis* (A.Massal.) Vězda (P-cB and B-cB) and, on P only, *Porina linearis*

(Leight.) Zahlbr. (P-cP). Nomenclature follows Smith *et al.* (2009). Freshly broken surfaces of the blocks were also considered as controls, representative of unweathered surfaces (d).

Four and five blocks were investigated for P and B, respectively (Figure 1), according to availability in the sampling sites of suitable blocks which hosted all the different colonization types. On each block, measuring areas were established for each colonization type (one surface of approx. 3 cm² for biofilm and freshly broken controls; one mature thallus for each species of epilithic and endolithic lichens). On each measuring area, measures were sequentially performed on: (i) surface hardness and (ii) water absorption capacity. Measures on areas colonized by lichens were repeated one day after the thalli were removed, as described below, to simulate the decay of senescent/dead thalli on natural outcrops and their cleaning on monumental surfaces. Additional measuring areas on each block were also established for each colonization type to characterize the lichen-rock interface by (iii) reflected light (RLM) and scanning electron (SEM) microscopy, and (iv) Raman spectroscopy.

The removal of the lichen thalli from the rock surfaces was carried out, after wetting the measuring areas, under a stereomicroscope. For epilithic lichens, the thalline areaolae (TC, sensu Favero-Longo *et al.*, 2005) were gently removed using a scalpel, leaving the medulla-rock interface intact. Endolithic lichen thalli were also gently scraped with a scalpel until the algal layer was exposed, substantially removing their lithocortex (sensu Pinna *et al.*, 1998). Repeated observations of representative cross-sectioned materials, before and after the removal of epilithic and endolithic thalli, confirmed that the defined procedures avoided causing mechanical damages detectable by RLM.

Reflected light and scanning electron microscopy

The growth of microbial biofilms on and/or below the rock surface, and the lichen-rock interface were examined under reflected light (RLM) and scanning electron (SEM) microscopy.

RLM observations were carried out by an Olympus SZH10 on cross sections (approx. 2-5 × 5-10 × 0.5 cm h × l × w, at least 3 sections per colonization type per block) cut with a diamond saw and stained using the periodic acid - Schiff (PAS) to visualize the biological component within the lithic substrate (Favero-Longo *et al.*, 2005). The profile of the lichen-rock interface (i.e. the structural organization of epilithic and endolithic lichens at the rock interface) was characterized by measuring thickness and depths of morphologically/physiognomically different layers at randomly selected vertical transects.

SEM observations were carried out by a Scanning Electron Microscope JEOL JSM IT300LV (High Vacuum - Low Vacuum 10/650 Pa - 0.3-30kV) on carbon-coated analogous cross sections and fracture samples to morphologically evaluate the hyphal-mineral interactions at the different layers of the lichen-rock interface. Images acquired in back-scattered (BSE) modes (BED-C and BED-S) were also acquired, on representative cross-sections for the different colonization types, to visualize the ratio between granules (light grey-coloured in BSE) and voids including grain boundaries, pores and cracks (porosity sensu lato, s.l., black coloured in BSE) in fresh parts of the lithotypes and at the lichen interface (Sardini *et al.*, 2006; Favero-Longo *et al.*, 2009). Images were processed by a pixel-based colour classification using the software ImageJ 1.50i (National Institutes of Health, Bethesda, Maryland, USA). Cross sections and fracture samples are conserved in the Lichen-Petrographic Collection of the Herbarium of the University of Torino (Gazzano *et al.*, 2007).

Raman spectroscopy

Raman spectra were collected at the different layers of the lichen-rock interface with a micro-spectrometer Horiba Jobin-Yvon HR800 equipped with an HeNe laser at an excitation wavelength of 632.8 nm, a CCD air-cooled detector operating at -70°C, and an Olympus BX41 light microscope. The spectra were compared with those contained in the Raman Spectra Database of Minerals and Inorganics and in Bernstein *et al.* (2002), Edwards *et al.* (2003) and Casanova-Municchia *et al.* (2014).

Karsten tube

A Karsten tube, a small open-ended glass vial, was attached to the rock face using a sealant compound based on plastic (Plastic-Fermit white; Fermit: Vettelschoß, Germany) to measure water penetration (Mol and Viles, 2012). By measuring the decrease in water level (Δ) in the tube over a period of four hours, the water absorption per square centimetre of rock surface was calculated. Measurements were taken every 5 minutes for the duration of the 240 minutes' infiltration time and recorded as ml/7.065 mm² min (infiltration surface of the Karsten tube, manufacturer's specifications). For each measuring area (i.e. colonization type x block, before and after removal procedures), measurements were replicated five times, each measure being performed after the absence of residual moisture had been verified with a CEM-dt 128 Pinless Moisture Meter (Shenzhen Everbest Machinery Industry Co., China) and, in any case, at least after one day. The three most consistent absorption curves were used for calculating average values of

$$(\Delta t_n - \Delta t_0)/A \text{ (eq. 2)}$$

at $t_n = 15 \text{ min } (t_1), 30 \text{ min } (t_2), 60 \text{ min } (t_3), 120 \text{ min } (t_4) \text{ and } 240 \text{ min } (t_5)$, with $t_0 = 0 \text{ min}$.

Average values of

$$(\Delta_{t+10\text{min}} - \Delta_t)/A \text{ (eq. 3)}$$

were also calculated for $t = 5 \rightarrow 230$ min, and used to calculate the average absorption rate for each ten minutes interval between the different time points (t_n and t_{n+1}).

Differences among the overall colonization types and between-types differences were tested applying non-parametric statistics Kruskal-Wallis and Mann-Whitney U Test, respectively, using Systat 10.2 (SYSTAT, Evanston, IL, USA). The data were visualized as boxplots obtained using RStudio (version 0.99.489 - © 2009-2015 RStudio, Inc.).

Equotip

Variability in block surface hardness was measured using a Proceq Equotip Piccolo 2, DL-type (Proceq, Switzerland), a rock surface hardness rebound device ideal for use on soft and weathered surfaces (Viles *et al.*, 2011; Wilhelm *et al.*, 2016a). In the Equotip Piccolo 2, a 2.78 mm diameter spherical tungsten carbide test tip is mounted in an impact body and impacts at 11.1 N mm under spring force against the test surface from which it rebounds. The DL probe (tungsten carbide, 2.78 mm) was used as it is able to obtain readings in confined spaces and thus suited the sometimes rough surfaces. The velocity before impact (V_1) and after impact (V_2) are measured automatically and displayed as a ratio ($V_2/V_1 \times 1000$) which is denoted by the Leeb Hardness (HL) unit (measuring range: 250-970 HLDL using the DL probe).

For each measuring area (colonization type x block), a combination of two measuring procedures [single impact method (SIM) and repeated impact method (RIM)] was adopted to provide a more robust evaluation of surface hardness characteristics (Yilmaz, 2013; Wilhelm *et al.*, 2016b). A series of 45 randomly distributed readings (SIM; for a confidence level of 95%) was firstly carried out to evaluate the elastic and plastic properties of the rock surfaces covered by the different colonization types. A second series of 20 repeated measurements (RIM) on five points was then taken to characterize the elastic and plastic properties of the surface and subsurface of the colonized rock, reflecting strength

characteristics such as the consolidation of mineral grains, the looseness of the original rock surface, and the degree of compaction due to repeated impacts (Aoki and Matsukura, 2007). After the removal of lichen thalli, a third series of randomly distributed readings (SIM) and a fourth one of repeated measurements (RIM) were analogously carried out to evaluate the rock hardness below/after the removal or scraping of the thalline component and lithocortex for epilithic and endolithic lichens, respectively.

The median value of the SIM series ($HLDL_{S,med}$) and the median of the maximum values of the five RIM series ($HLDL_{R,med}$) were used to calculate for each measuring area the robust hybrid dynamic hardness (HDH_{robust} , sensu Wilhelm *et al.*, 2016b) as follows:

$$HDH_{robust} = (HLDL_{S,med})^2 / (HLDL_{R,med}) \text{ (eq. 1)}$$

Differences among the overall colonization types and between-types differences were tested applying non-parametric statistics Kruskal-Wallis and Mann-Whitney U Test, respectively, using Systat 10.2 (SYSTAT, Evanston, IL, USA). The data were visualized as boxplots obtained using RStudio (version 0.99.489 - © 2009-2015 RStudio, Inc.).

Results

Microscopy and Raman spectroscopy at the lichen-rock interface

RLM observations on cross sections showed for all epilithic and endolithic lichen species a stratified interface with the underlying substrate, developed from the surface into the interior of Portland (Figure 2) and Botticino (Figure 3) limestones. By contrast, the investigated microbial biofilms mostly grew epilithically on the calcareous surfaces, poor penetration of associated hyphal structures being only sporadically observed (Figures 2a-b, 3a-b).

The following lichen-rock interface layers were recognized, which were present or absent depending on the species and on the colonized lithology (Table 1): lithocortex (LI, sensu Pinna *et al.*, 1998), endolithic photobiont layer (PL, sensu Pinna *et al.*, 1998), pervasive (pHPC) and sparse (sHPC) hyphal penetration component (sensu Favero-Longo *et al.*, 2005, equivalent for endolithic species to the pseudomedulla layer, sensu Pinna *et al.*, 1998). The lichen-rock interface organization mostly varied among species with regard to the presence/absence of LI and PL layers and on the thickness and depths of pHPC and sHPC layers (Table 1; additional photographic profiles of the lichen-rock interface in Supplementary material 1). Each species generally showed a similar organization on the two lithotypes with regard to LI, PL and pHPC layers, while sHPC layer was generally negligible in Botticino.

In particular, cross sections showed that *Caloplaca marina* and *C. ochracea* (Figures 2c-d, 3c-d) discontinuously developed a 100-300 μm thick epilithic thalline component (sensu Favero-Longo *et al.*, 2005), including photobionts, or a 100-200 μm thick endolithic PL (sensu Pinna *et al.*, 1998) immersed beneath a crystalline film. Beneath these upper “alternative” layers, both the lithotypes were penetrated by an approx. 100-300 μm thick pHPC, followed by a sHPC down to a depth of approx. 1.0 mm. Beneath its truly epilithic

thalli, *Verrucaria nigrescens* (Figures 3e-f) developed a thicker pHPC (approx. 600-800 μm), while a deeper sHPC was poorly observed.

Both *Bagliettoa baldensis* (Figures 2g-h, 3g-h) and *Porina linearis* (Figures 2e-f) developed truly endolithic thalli with a 70-150 μm thick immersed PL, but remarkably differed for the presence of a prominent 50-100 μm thick LI (sensu Pinna *et al.*, 1998) in the former species (Figure 4a). Beneath the PL, the pHPC of *Bagliettoa baldensis* penetrated the Portland and Botticino limestones down to depths of approx. 300-700 μm and 150-400 μm , respectively. A sHPC was observed in Portland down to depths of approx. 2.0-3.0 mm, while it was scarce in Botticino. *Porina linearis* developed pHPC within the Portland limestone down to 300-1200 μm , while a deeper, sHPC was observed down to 2.0-3.0 mm. For all the species, diffuse PAS staining at the pHPC level likely indicated an abundance of extracellular polymeric substances (EPS), which were instead less detected at the other layers.

RLM observations on Portland revealed at the interface with the different species a loss of the oolitic appearance down to depths of approx. 100-500 μm , while a lower layer, down to 700-1000 μm , still showed its oolitic structure, but darker hues. At the lichen-Botticino interface some colour shift was observed down to 300-500 μm , but the rock microstructure was unmodified.

SEM observations highlighted at the different interface layers the hyphal organization and localization with respect to the mineral component, clarifying differences between the endolithic lichen species on Portland. BSE mode observations at the LI and PL of *B. baldensis* displayed a poor signal of the mineral component, indicating dominance of voids occupied by the biotic component (porosity s.l., observed by BSE imaging, over than 50%; Figure 4b). Conglutination of hyphae and microcrystals was another prominent feature at these layers (Figure 4c). Beneath LI and PL, a decreasing of voids at increasing distance from the surface was recognizable (porosity s.l. at the PL-LI >> pHPC >> sHPC >

1 uncolonized layer and freshly broken controls; Figure 4b and Supplementary material 2).
2
3
4 In *P. linearis*, photobionts were sparse in the early 150 μm beneath the surface (Figure
5
6 4d), where the oolitic structure was masked (Figures 4e-f). At the pHPC layer, penetrating
7
8 hyphae were strictly intermingled with microcrystals (Figures 4g-h). Beneath this layer,
9
10 hyphae were more sparsely observed, but occurred densely within wider rock
11
12 discontinuities (Figure 4i). A similar interface structure also characterized *C. marina* in
13
14 Portland. By contrast, in the case of *C. ochracea* and *B. baldensis* within Botticino, the
15
16 hyphal occurrence beneath the algal layer was mostly related with the local occurrence of
17
18 wide discontinuities (Figure 4l). BSE observations on lichen species on Botticino confirmed
19
20 the pervasive, but shallow HPC development beneath the surface, where the increase of
21
22 dark colours indicated a lichen-related increased porosity down to 600-800 μm in depth
23
24 (e.g. porosity s.l., observed by BSE imaging, at the pHPC of *V. nigrescens* >> uncolonized
25
26 layer > freshly broken controls; Figure 4m and Supplementary material 2).
27
28

29
30 Raman spectroscopy at the lichen-rock interface of all the endolithic and epilithic species
31
32 consistently displayed spectra attributable to calcite, while oxalates were never detected.
33
34 At the LI and PL layers of endolithic species, spectral bands with wavenumber at 1520 and
35
36 1161 cm^{-1} , assignable to C=C and C-C stretching modes, respectively, and likely
37
38 attributable to carotenoids (Bernstein *et al.*, 2002; Casanova-Municchia *et al.*, 2014) were
39
40 also observed, while only the calcite vibrational modes were detected at the deeper layers
41
42 and in the bulk (Supplementary material 3).
43
44
45

46 47 48 49 *Water absorption capacity*

50
51 Karsten tube measurements showed different absorption capacities of limestone surfaces
52
53 affected by the different colonization types, and a general increase of absorption capacity
54
55 of surfaces colonized by lichens after the removal and scraping of epilithic and endolithic
56
57 thalli, respectively (Figure 5; Supplementary material 4).
58
59
60

On both lithologies and for all the colonization types, higher absorption rates were detected at the t_0 - t_1 and t_1 - t_2 intervals, while values (and variability) progressively decreased and became stable at the successive measuring intervals. Different colonization types, however, displayed different effects on the absorption patterns. On Portland (Figure 5), both rate and cumulative values showed significantly higher absorption for surfaces colonized by *B. baldensis*, before and after the scraping, and *P. linearis* after the scraping, with respect to those colonized by microbial biofilms and *Porina linearis* before the scraping. Surfaces colonized by *C. marina* also showed low values, but thalli on the examined blocks did not allow enough measurements to be collected to run statistical analyses. On Botticino (Supplementary material 4), surfaces colonized by *B. baldensis*, before and after the scraping, and *C. ochracea* and *V. nigrescens*, after thallus removal, showed higher absolute values of water absorption, but also in this case only a limited set of reliable data was collected because deep internal cracks often compromised measures, preventing any statistical analyses.

Hybrid dynamic hardness

Equotip measurements showed that some of the epilithic and endolithic lichens affected the hardness of the Portland and Botticino surfaces when compared to controls. Although a high spread of values was detected for some study cases, the hybrid dynamic hardness (HDH_{robust} ; Figure 6) and the hardness measured by single impact method ($HLDL_S$) (Supplementary material 6) of surfaces colonized by lichens was generally lower than that of exposed surfaces with microbial biofilms only and of freshly broken ones. In contrast, higher HDH_{robust} and $HLDL_S$ values characterized the same surfaces after the removal of thalline component and scraping of lithocortex for epilithic and endolithic species, respectively. Hardness measured by repeated impact method ($HLDL_R$) was rather steady before and after removal and scraping procedures (Supplementary material 6).

Portland surfaces colonized by *B. baldensis* showed, in particular, significantly lower HDH_{robust} and $HLDL_S$ values than all the other colonization types. On Botticino, the lowest average values were obtained when Equotip was applied on the thick and thin epilithic thalli of *V. nigrescens* and *C. ochracea*, respectively, while surfaces colonized by *B. baldensis* displayed HDH_{robust} and $HLDL_S$ values slightly lower than those with epilithic biofilms.

After the scraping or removal procedures, Portland and Botticino surfaces differed in the fact that the former generally showed HDH_{robust} and $HLDL_S$ values higher than those of controls (freshly broken surfaces and surfaces with microbial biofilms only), while the latter showed values similar to those of controls.

Discussion

By combining the microscopical characterization of lichen-limestone interface with direct measures of water absorption capacity and hardness, this study illustrates how lichen colonization of the surface and interior of limestones affects physical properties potentially relevant for durability. Specific structural organizations of epilithic and endolithic lichens on/within the rocks were associated to differential patterns of water absorption increase with respect to surfaces with microbial biofilms, even more pronounced after the removal or scraping of their upper structural layers (thalline component and lithocortex for epilithic and endolithic species, respectively). Increased water absorption was likely related to the absorption behaviour of intact thalli and the within-rock discontinuities penetrated by hyphae, more exposed after the removal or scraping procedures. However, measures by Equotip, informative on elastic and plastic properties of stone surfaces and subsurfaces, and proxy of open porosity (Wilhelm *et al.*, 2016b), revealed another related scenario. Only surfaces bearing intact thalli showed lower values of hybrid dynamic hardness (HDH_{robust}), related to compressibility, and hardness measured by single impact method ($HLDL_S$) with

respect to control surfaces, freshly broken or colonized by microbial biofilms. By contrast, after the removal or scraping procedures, the HDH_{robust} and $HLDL_S$ values were similar or higher than those of controls, suggesting that a biogenic hardening process may accompany the increasing open porosity. In the following sub-sections, we discuss the recognized structural layers of epilithic and endolithic lichen-limestone interface (*Structural organization of the lichen-rock interface*) to support the understanding of correlations between lichen colonization and limestone physical properties (*Lichen influence on the physical properties of limestones and weathering*).

Structural organization of the lichen-rock interface

Microscopic investigations have found differential layered arrangements of the lichen-rock interface within a wide set of lithologies (de los Ríos and Ascaso, 2005; Favero-Longo *et al.*, 2005; Casanova-Municchia *et al.*, 2014). Specific structural layers observed for the examined epilithic and endolithic lichens, recognized within both the Portland and Botticino limestones, were consistent with reports on several carbonate lithologies for the same species and/or others with similar functional traits and ecological requirements (Pinna *et al.*, 1998; Bungartz *et al.*, 2004; Hoppert *et al.*, 2004; Favero-Longo *et al.*, 2009; McIlroy de la Rosa *et al.*, 2012). In the endolithic *Bagliettoa baldensis* and *Porina linearis*, the development of fruiting bodies was remarkably associated with pitting phenomena, widely recognized as a prominent effect of endolithic lichens on carbonate rocks (Salvadori and Casanova Municchia, 2016). The thickness ranges of PL were analogous to the dataset of Pinna *et al.* (1998), as related to the light harvesting capacity. Microscopy and Raman analyses displayed for *B. baldensis* an upper lithocortex, composed of fine-grained calcite surrounding sparse hyphae. Such a layer, less prominent in *P. linearis*, morphologically resembled the fine-grained micrite layer described for the endolithic *Verrucaria rubrocincta* on caliche limestone (Bungartz *et al.*, 2004), and recognized as a biomineralization

product by isotope analyses (Garvie *et al.*, 2008). Depths of pHPC, ranging from few hundreds of microns to approx. 1 mm, differed between species (Pinna *et al.*, 1998), but were also more related to the two lithotypes. Higher total porosity of Portland limestone, confirmed for the sample set with SEM-BSE observations, likely favoured a more extensive development of pHPC and the occurrence of a sHPC down to depths of 2-4 mm, which was scarce in the less porous Botticino. Differences in type and extent of porosity s.l. have indeed been recognized as relevant factors to determine the extent of fungal colonization within sedimentary rocks (Cámara *et al.*, 2008). On the other hand, the rock volume penetrated by the sHPC displayed an increase of porosity s.l. (secondary porosity) with respect to the deeper layers, according to the active dissolution processes related to the growth of endolithic lichens (Salvadori and Casanova-Municchia, 2016). In Portland, this pattern was related to a pronounced hyphal intragranular penetration and the loss of the oolitic appearance, also observed in other oolitic limestones penetrated by Verrucariaceae (Concha-Lozano *et al.*, 2012). Presence of oxalates, debated with regard to the endolithic lichen-rock interface (Bungartz *et al.*, 2004), was not observed here, according to previous findings of Pinna *et al.* (1998).

The areolate thalline component of *Verrucaria nigrescens*, displaying a truly epilithic structure, was associated with a thick pHPC down to 800 μm , compatible to the range of depths reported for the same species in other carbonate lithologies (Favero-Longo *et al.*, 2009). The *Verrucaria* pHPC layer displayed higher porosity with respect to uncolonized deeper layers, suggesting lichen related dissolution processes (Cámara *et al.*, 2008; Favero-Longo *et al.*, 2009).

Although *Caloplaca ochracea* has been reported as epilithic (Smith *et al.*, 2009), anatomical observation of the cross-sectioned discontinuous thalli confirmed previously recognized difficulties in classifying its growth form (Pinna *et al.*, 1998) and reports as endolithic species (Nimis and Martellos, 2008). Our observations disclosed similar issues

for *C. marina*. As the thalline component (TC) was discontinuously present, wide parts of the thalli were immersed within the limestones, showing a layered structure similar to the truly endolithic *B. baldensis* (LI-PL-HPC).

Lichen influence on the physical properties of limestones and weathering

The data collected with Karsten tube and Equotip on lichen-covered, microbial biofilm-covered and freshly broken surfaces allow directly comparable observations of the physical properties of limestones with and without lichen cover. In some cases (in particular for Botticino), the rock blocks selected for analyses finally revealed a restricted availability of surfaces colonized by lichens suitable to run the time-consuming Karsten-tube measures (5 measures of 4 hours per sample replicate with operator's check-times of 5 min), limiting the collection of a dataset suitable for statistical analyses. Nevertheless, our findings offer a first experimentally-supported insight on the influence of epilithic and endolithic lichens on the water absorption capacity of limestones and their hardness response to single and repeated impacts.

On both Portland and Botticino, our analyses showed the highest water absorption values on surfaces colonized by the LI-bearing *Bagliettoa*, while those of epilithic species, *Porina linearis* (without a prominent LI-layer), and the microbial biofilms were rather similar. Epilithic lichens, in particular *Verrucaria nigrescens*, have been shown to retain moisture on limestone (Saint Quentin) surfaces (Carter and Viles, 2003) and have been suggested to play an umbrella-like protection with respect to deteriorogenic endolithic species, as *Bagliettoa baldensis* (Carter and Viles, 2005). By contrast, occurrence of *Bagliettoa baldensis* on Burren limestone has been shown to reduce dissolution processes if compared to bare surfaces (McIlroy de la Rosa *et al.*, 2014). Similarly, a surface-sealing effect of the lithocortex of *Verrucaria rubrocincta*, anatomically similar to the LI of examined species, has also been hypothesized on Sonoran caliche limestone (Bungartz *et*

1
2
3
4
5
6
7
8
9
10
11
12
13
14
15
16
17
18
19
20
21
22
23
24
25
26
27
28
29
30
31
32
33
34
35
36
37
38
39
40
41
42
43
44
45
46
47
48
49
50
51
52
53
54
55
56
57
58
59
60

al., 2004). Our observations showed an increase in water absorption after the removal/scraping procedures, which likely removed the sealing effect and made accessible the primary porosities and the secondary ones related to pHPC, shown by SEM-BSE observations. A similar loss of water-proofing effect of endolithic Verrucariaceae on oolitic limestones has been reported after sandblasting and calcification of surfaces, but poorly related to the lichen structural features (Concha-Lozano *et al.*, 2012).

Combination of single and repeated impact measures with Equotip showed lower $HLDL_S$ and HDH_{robust} values for surfaces bearing intact thalli than freshly broken and microbial colonized controls. These values were respectively related to hardness and compressibility of the biological (thalline component) or biomineralized (lithocortex) layers with respect to the mineral ones, on which they have a cushion-like effect. Similar results have been found in Antarctica where hardness measures on lichens gave lower values than bare surfaces when carried out directly on epilithic thalli (Guglielmin *et al.*, 2012). After the removal and scraping of upper layers, and the exposure of secondary porosity, as revealed by Karsten tube, $HLDL_S$ and HDH_{robust} values were similar (Botticino) or even higher (Portland) than those of controls. Although the rock layers occupied by pHPC displayed higher porosity and exhibited a mineral-leached structure, their elastic and plastic properties appeared improved with respect to freshly broken and microbial biofilm controls. Such findings support the recent hypothesis that lichens were responsible for higher hardness ($HLDL_S$) of uncleaned Portland headstones with respect to regularly cleaned ones (Wilhelm *et al.*, 2016b). As biogenic calcite of several biological systems, as seashells, was shown to display superior hardness, and model synthetic calcite crystals with contents of amino acids revealed enhanced hardness (Kim *et al.*, 2016), our results suggest the opportunity to investigate if and how hardening patterns may also accompany lichen biogeochemical processes on limestones.

1
2
3
4
5
6
7
8
9
10
11
12
13
14
15
16
17
18
19
20
21
22
23
24
25
26
27
28
29
30
31
32
33
34
35
36
37
38
39
40
41
42
43
44
45
46
47
48
49
50
51
52
53
54
55
56
57
58
59
60

Our observations have implications for the contribution of lichens to weathering of limestone in natural and cultural settings, as well as for the impacts of removing lichens from stone in cultural heritage. Lichen colonization has been proposed to contribute to the development of micro- and meso-scale weathering morphologies and to affect the overall rate of karstification (McIlroy de la Rosa *et al.*, 2012; McIlroy de la Rosa 2016). The suggested models, also supposing the potential succession of different communities during the long and complex surface histories, considered the lichen effect on a timescale which is not compatible with direct observations (McIlroy de la Rosa *et al.*, 2013; Viles, 2012). In this work, influences of lichen colonization on the physical properties of Portland and Botticino limestones were considered during the presence of living thalli on/within the rocks and immediately after the removal or scraping of their upper structural layers, simulating their natural decay or cleaning work by restorers, and can thus contribute to evaluating and refining geomorphological models of lichen biomodification.

McIlroy de la Rosa *et al.* (2013) propose two models illustrating the short-term bioprotective role of lichens (with and without calcium oxalate encrustation) followed by episodic accelerated weathering when the thalline shielding and calcium oxalate encrustation effects are removed following death of the lichen. The findings in this study provide support for this sort of temporal sequence (through comparison of lichen-covered with freshly-broken surfaces), but reveal the importance of lichen-induced biogenic hardening in the absence of calcium oxalate precipitation as an additional factor not considered by McIlroy de la Rosa *et al.* (2013). Comparisons between microbial biofilm-covered, freshly broken and lichen-covered surfaces can also throw light on the third and fourth models of McIlroy de la Rosa *et al.* (2013), which address longer term evolution of karstic surfaces where dynamic relations between lichen biomodifications and dissolution processes are predicted. The findings in this study help refine and calibrate such models. Truly bare surfaces, with only abiotic dissolution, are highly unlikely in most natural karst

environments and thus using biofilm-covered surfaces as a control improves the model. Furthermore, findings such as harder surface characteristics and lower water penetration rates on microbial biofilm-covered surfaces indicate lower weathering rates than those produced by the net effect of lichen growth and decay (lichen-covered and freshly broken surfaces) in Portland and Botticino.

Conclusions

Lichens have variously been claimed to be biodeteriorative or bioprotective on rocks depending on lithologies and several other factors (Seaward, 2015; Salvadori and Casanova Municchia, 2016). On limestone, the hyphal penetration and surface biomineralization by endolithic *Verrucaria rubrocincta* has even been explained as simultaneous counter-balancing processes yielding deterioration and protection, respectively (Bungartz *et al.*, 2004). Our work was not limited to consider lichen development within rocks and biomineralization phenomena as proxies of deterioration or protection, but also related detailed observations of lichen-rock interactions with physical properties of limestone potentially relevant to durability and weathering, i.e. water penetration and surface hardness. Limestone substrate colonized by epilithic and endolithic lichen structures generally displayed an increased water absorption capacity due to lichen-induced secondary porosity, generally associated with increased stone decay (Karaca, 2010). By contrast, the lichen-rock interface revealed unmodified or even increased hardness of limestone, often related to higher durability (and lower weathering rates) of many different lithologies (Guglielmin *et al.*, 2012; Mol and Viles, 2012). Although such counterposed patterns should be still verified on a wider range of limestone lithologies in different (micro-)climate conditions, these findings need to be taken into account when models relating lichen occurrence on limestones and biogeomorphological surface evolution are proposed (McIlroy de la Rosa *et al.*, 2012, 2013). Our analyses,

indeed, confirmed the working hypothesis that limestones colonized by lichens display physical properties, such as hardness and water absorption, which are different from surfaces exposed to other abiotic and biotic weathering factors, likely influencing their morphological evolution. Moreover, the documented biogeomorphological significance of lichens appears diverse depending on the structural organization at the rock interface of the different epilithic and endolithic species. In general, however, deterioration related to hyphal penetration in limestone is likely counterbalanced by a parallel protective effect of lichens, which lasts while the rock surface is covered by thalline component and lithocortex of epilithic and endolithic species, respectively, which provide an umbrella-like effect and limit erosion processes. Subsequent decay/removal of the upper structural layers of lichens expose surfaces with higher permeability, but hardened, likely prone to flaking, as described for case-hardened siliceous surfaces (Dorn, 2013). The stability of natural limestone surfaces may be thus in part related to the persistence of lichen communities. Future research should verify whether and, if so, which other weathering processes may follow the potential decay of the hyphal penetration component and the ecological succession of other microbial lithobionts in the endolithic microniche previously occupied by lichens. Environmental variations related to global change dynamics potentially affecting lichen communities and their decay rate may indirectly affect the geomorphological dynamics, even before being directly effective on them (see Viles and Cutler, 2012). In particular, differential effects on limestone physical properties recorded for different epilithic and endolithic species imply that equilibria between lichen communities and biogeomorphological dynamics may be mediated by the selective responses of each species to environmental pressures. Finally, the fact that limestone surfaces colonized by lichens become a biogeomaterial with peculiar physical properties, modified with respect to the fresh stone, should be considered when policies of

conservation or removal of lichen cover from the stone cultural heritage have to be established.

Acknowledgements

MM is a recipient of a doctoral fellowship funded by INPS (Istituto Nazionale di Previdenza Sociale, Italy). The authors are grateful to the Editor in Chief, Prof. Stuart N. Lane, and two anonymous reviewers for helpful and constructive comments, to Consorzio Produttori Marmo Botticino Classico for access to the quarry area and to Mona Edwards and Hong Zhang (Oxford Rock Breakdown Laboratory, University of Oxford) for technical assistance. MM particularly thanks Vanessa Winchester (University of Oxford) for precious discussions on British lichens.

References

- Adamo P, Violante P. 2000. Weathering of rocks and neogenesis of minerals associated with lichen activity. *Applied Clay Science* **16**: 229-256.
- Aoki H, Matsukura Y. 2007. A new technique for non-destructive field measurement of rock-surface strength: an application of the Equotip hardness tester to weathering studies. *Earth Surface Processes and Landforms* **32**: 1759-1769.
- Barker WW, Banfield JF. 1996. Biologically versus inorganically mediated weathering reactions: relationships between minerals and extracellular microbial polymers in lithobiontic communities. *Chemical Geology* **132**: 55-69.
- Bernstein PS, Zhao DY, Wintch SW, Ermakov IV, McClane RW, Gellermann W. 2002. Resonance Raman measurement of macular carotenoids in normal subjects and in age-related macular degeneration patients. *Ophthalmology* **109**: 1780-1787.
- Borghi A, Berra V, d'Atri A, Dino GA, Gallo LM, Giacobino E, Martire L, Massato G, Vaggelli G, Bertok C, Castelli D, Costa E, Ferrando S, Groppo C, Rolfo F. 2015. Stone

- materials used for monumental buildings in the historical centre of Turin (NW Italy): Architectonical survey and petrographic Characterization of Via Roma. *Geological Society, London, Special Publications* **407**: 201–18.
- Brunsdon D, Coombe K, Goudie AS, Parker AG. 1996. The structural geomorphology of the Isle of Portland, southern England. *Proceedings of the Geologists' Association*, **107**: 209-230.
- Bungartz F, Garvie LAJ. 2004. Anatomy of the endolithic Sonoran Desert lichen *Verrucaria rubrocincta* Breuss: implications for biodeterioration and biomineralization. *Lichenologist* **36**: 55-73.
- Cámara B., De los Ríos A, García del Cura MA, Galván V, Ascaso C. 2008. Dolostone bioreceptivity to fungal colonization. *Materiales de Construcción* **58**: 113-124.
- Carter NEA, Viles HA. 2005. Bioprotection explored: the story of a little known earth surface process. *Geomorphology* **67**: 273-81.
- Carter NEA, Viles HA. 2004. Lichen hotspots: raised rock temperatures beneath *Verrucaria nigrescens* on limestone. *Geomorphology* **62**: 1-16.
- Carter NEA, Viles HA. 2003. Experimental investigations into the interactions between moisture, rock surface temperatures and an epilithic lichen cover in the bioprotection of limestone. *Building and Environment* **38**: 1225-34.
- Casanova Municchia AG, Caneva G, Ricci MA, Sodo A. 2014. Identification of endolithic traces on stone monuments and natural outcrops: preliminary evidences. *Journal of Raman Spectroscopy* **45**: 1180-1185.
- Chen J, Blume H-P, Beyer L. 2000. Weathering of rocks induced by lichen colonization-a review». *Catena* **39**: 121-146.
- Concha-Lozano N, Gaudon P, Pages J, de Billerbeck G, Lafon D, Eterradosi O. 2012. Protective effect of endolithic fungal hyphae on oolitic limestone buildings. *Journal of Cultural Heritage* **13**: 120–27.

- De los Rios A, Ascaso C. 2005. Contributions of in situ microscopy to the current understanding of stone biodeterioration. *International Microbiology* **8**: 181-188.
- Dorn RI. 2013. Rock coatings. In Treatise on Geomorphology, vol. 4, Weathering and Soils Geomorphology, Shroder J, Pope GA (eds). Academic Press: San Diego (USA); 70-97.
- Dubelaar CW, Engering S, Van Hees RPJ, Koch R, Lorenz HG. 2003. Lithofacies and petrophysical properties of Portland Base Bed and Portland Whit Bed limestone as related to durability. *Heron* **48**: 221-229.
- Edwards HG, Seaward MR, Attwood SJ, Little SJ, de Oliveira LF, Tretiach M. 2003. FT-Raman spectroscopy of lichens on dolomitic rocks: an assessment of metal oxalate formation. *Analyst* **128**: 1218-1221.
- Favero-Longo SE, Accattino E, Matteucci E, Borghi A, Piervittori R. 2015. Weakening of gneiss surfaces colonized by endolithic lichens in the temperate climate area of northwest Italy. *Earth Surface Processes and Landforms* **40**: 2000-2012.
- Favero-Longo SE, Gazzano C, Girlanda M, Castelli D, Tretiach M, Baiocchi C, Piervittori R. 2011. Physical and chemical deterioration of silicate and carbonate rocks by meristematic microcolonial fungi and endolithic lichens (Chaetothyriomycetidae). *Geomicrobiology Journal* **28**: 732-744.
- Favero-Longo SE, Borghi A, Tretiach M, Piervittori R. 2009. In vitro receptivity of carbonate rocks to endolithic lichen-forming aposymbionts. *Mycological research* **113**: 1216-1227.
- Favero-Longo SE, Castelli D, Salvadori O, Belluso E, Piervittori R. 2005. Pedogenetic action of the lichens *Lecidea atrobrunnea*, *Rhizocarpon geographicum* gr. and *Sporastatia testudinea* on serpentinized ultramafic rocks in an alpine environment. *International Biodeterioration & Biodegradation* **56**: 17-27.

- Garvie LA, Knauth LP, Bungartz F, Klonowski S, Nash III TH. 2008. Life in extreme environments: survival strategy of the endolithic desert lichen *Verrucaria rubrocincta*. *Naturwissenschaften* **95**: 705-712.
- Gazzano C, Favero-Longo SE, Matteucci E, Roccardi A, Piervittori R. 2009. Index of Lichen Potential Biodeteriogenic Activity (LPBA): a tentative tool to evaluate the lichen impact on stonework. *International Biodeterioration & Biodegradation* **63**: 836-843.
- Gazzano C, Favero-Longo SE, Matteucci E, Castelli D, Piervittori R. 2007. Allestimento di una collezione licheno-petrografica presso l'Erbario Crittogamico di Torino per lo studio del biodeterioramento di rocce e materiali lapidei. In *Lo stato dell'arte 5: V Congresso nazionale IGIIIC: Cremona, 11-13 ottobre 2007*. Nardini: Firenze; 669-677.
- Golubic S, Friedmann I, Schneider J. 1981. The lithobiontic ecological niche, with special reference to microorganisms. *Journal of Sedimentary Research* **51**: 475-478.
- Gorbushina AA, Broughton WJ. 2009. Microbiology of the atmosphere-rock interface: how biological interactions and physical stresses modulate a sophisticated microbial ecosystem. *Annual Review of Microbiology* **63**: 431-450.
- Guglielmin M, Worland MR, Convey P, Cannone N. 2012. Schmidt Hammer studies in the Maritime Antarctic: application to dating Holocene deglaciation and estimating the effects of macrolichens on rock weathering. *Geomorphology* **155-56**: 34-44.
- Hoppert M, Flies C, Pohl W, Günzl B, Schneider J. 2004. Colonization strategies of lithobiontic microorganisms on carbonate rocks. *Environmental Geology* **46**: 421-428.
- Jones D. 1988. Lichens and pedogenesis. In *Handbook of lichenology, Volume 3*, Galun M (ed). CRC Press: Boca Raton (USA); 109-124.
- Karaca Z. 2010. Water absorption and dehydration of natural stones versus time. *Construction and Building Materials* **24**: 786-790.
- Kim YY, Carloni JD, Demarchi B, Sparks D, Reid DG, Kunitake ME, Tang CC, DUER MJ, Freeman CL, Pokroy B, Penkman K, Harding JH, Estro LA, Baker SP, Meldrum FC.

2016. Tuning hardness in calcite by incorporation of amino acids. *Nature materials* 15: 903-910.
- Kip N, van Veen JA. 2015. The dual role of microbes in corrosion. *The ISME Journal* 9: 542-551.
- Matthews JA, Owen G. 2008. Endolithic lichens, rapid biological weathering and Schmidt hammer r-values on recently exposed rock surfaces: Storbreen glacier foreland, Jotunheimen, Norway». *Geografiska Annaler: Series A, Physical Geography* 90: 287-97.
- McCarroll D, Viles H. 1995. Rock-weathering by the lichen *Lecidea auriculata* in an arctic alpine environment. *Earth Surface Processes and Landforms* 20: 199-206.
- McIlroy de la Rosa, JP. 2016. The Burren: a glacial, karstic and biokarstic expression of a limestone plateau in western Ireland. *Earth Surface Processes and Landforms* 41: 1614-1628.
- McIlroy de la Rosa, JP, Warke PA, Smith BJ. 2012. Microscale biopitting by the endolithic lichen *Verrucaria baldensis* and its proposed role in mesoscale solution basin development on limestone: the role of *Verrucaria baldensis* in solution basin development". *Earth Surface Processes and Landforms* 37: 374-384.
- McIlroy de la Rosa JPM, Warke PA, Smith BJ. 2013. Lichen-induced biomodification of calcareous surfaces: bioprotection versus biodeterioration. *Progress in Physical Geography* 37: 325-351.
- McIlroy de la Rosa JP, Warke PA, Smith BJ. 2014. The effects of lichen cover upon the rate of solutional weathering of limestone. *Geomorphology* 220: 81-92.
- Mihajlovski A, Seyer D, Benamara H, Bousta F, Di Martino P. 2015. An overview of techniques for the characterization and quantification of microbial colonization on stone monuments. *Annals of Microbiology* 65: 1243-1255.

- Mol L, Viles HA. 2012. The role of rock surface hardness and internal moisture in tafoni development in sandstone: internal moisture and tafoni development in sandstone. *Earth Surface Processes and Landforms* **37**: 301-314.
- Nimis PL, Martellos S. 2008: *ITALIC - The Information System on Italian Lichens*. Version 4.0. University of Trieste, Dept. of Biology, IN4.0/1 (<http://dbiodbs.univ.trieste.it/>). Accessed on 15th September 2016.
- Pinna D, Salvadori O, Tretiach M. 1998. "An anatomical investigation of calcicolous endolithic lichens from the Trieste Karst (NE Italy). *Plant Biosystems* **132**: 183-195.
- Salvadori O, Casanova Municchia A. 2016. The Role of Fungi and Lichens in the Biodeterioration of Stone Monuments. *The Open Conference Proceedings Journal* **7**: 39–54.
- Sardini P, Siitari-Kauppi M, Beaufort D, Hellmuth KH. 2006. On the connected porosity of mineral aggregates in crystalline rocks. *American Mineralogist* **91**: 1068-1080.
- Scheerer S, Ortega-Morales O, Gaylarde C. 2009. Microbial deterioration of stone monuments - An updated overview. *Advances in Applied Microbiology* **66**: 97–139.
- Seaward MRD. 2015. Lichens as agents of biodeterioration. In *Recent Advances in Lichenology, Volume 1*, Upreti DA, Divakar PK, Shukla V, Bajpai (eds). Springer India:New Dehli; 189-211.
- Smith CW. 2009. *Lichens of Great Britain and Ireland*. British Lichen Society: London.
- St. Clair LL, Seaward MRD. *Biodeterioration of stone surfaces. Lichens and biofilms as weathering agents of rocks and cultural heritage*. Kluwer Academic Publishers, Dordrecht.
- Tiano P. 2016. Biodeterioration of stone monuments: a worldwide Issue». *The Open Conference Proceedings Journal* **7**: 29-38.
- Viles HA. 2012. Microbial geomorphology: a neglected link between life and landscape. *Geomorphology* **157-158**: 6-16.

- Viles HA, Cutler NA. 2012. Global environmental change and the biology of heritage structures. *Global Change Biology*, **18**: 2406-2418.
- Viles H, Goudie A, Grab S, Lalley J. 2011. The use of the Schmidt Hammer and Equotip for rock hardness assessment in geomorphology and heritage science: a comparative analysis. *Earth Surface Processes and Landforms* **36**: 320–33.
- Villar SE, Edwards HGM, Seaward MRD. 2004. Lichen biodeterioration of ecclesiastical monuments in Northern Spain. *Spectrochimica Acta Part A: Molecular and Biomolecular Spectroscopy* **60**: 1229–37.
- Wierzchos J, Ascaso C. 1994. Application of back-scattered electron imaging to the study of the lichen-rock interface. *Journal of Microscopy* **175**: 54–59.
- Wierzchos J, Ascaso C. 1998. Mineralogical transformation of bioweathered granitic biotite, studied by HRTEM: evidence for a new pathway in lichen activity. *Clays and Clay Minerals* **46**: 446-452.
- Wilhelm K, Viles H, Burke O. 2016a. Low impact surface hardness testing (Equotip) on porous surfaces - advances in methodology with implications for rock weathering and stone deterioration research: Equotip hardness testing on porous rock and stone». *Earth Surface Processes and Landforms* **41**: 1009-1152.
- Wilhelm K, Viles H, Burke O, Mayaud J. 2016b. Surface hardness as a proxy for weathering behaviour of limestone heritage: a case study on dated headstones on the Isle of Portland, UK. *Environmental Earth Sciences* **75**, 1-16.
- Yilmaz NG. 2013. The influence of testing procedures on uniaxial compressive strength prediction of carbonate rocks from Equotip Hardness Tester (EHT) and proposal of a new testing methodology: hybrid dynamic hardness (HDH). *Rock Mechanics and Rock Engineering* **46**: 95-106.

Figure captions

Figure 1. Lithobiont colonization types examined on Portland (P) and Botticino (B) limestones. Measurements of water absorption capacity and hardness were carried out by Karsten tube and Equotip on block surfaces, while the thickness and depth of the thalline (TC) and hyphal penetration (HPC) components (sensu Favero-Longo *et al.*, 2005) of epilithic and endolithic lichens were examined on cross-sectioned profiles. Study cases are schematically summarized on the right picture side: (a) epilithic microbial biofilm on Portland (P-a) and Botticino (B-a); (b) epilithic lichens on Portland, *Caloplaca marina* (P-bC), and on Botticino, *Caloplaca ochracea* (B-bC) and *Verrucaria nigrescens* (B-bV); (c) endolithic lichens on Portland, *Porina linearis* (P-cP) and *Bagliettoa baldensis* (P-cB), and on Botticino, *Bagliettoa baldensis* (B-cB); d-freshly broken surfaces of Portland (P-d) and Botticino (B-d).

Figure 2. Lithobiont growth within the Portland limestone (cross sections observed under RLM before –a,c,d,g- and after – b,d,f,h – staining by PAS): (a, b) epilithic microbial biofilm; (c, d) *Caloplaca marina*; (e, f) *Porina linearis*; (g, h) *Bagliettoa baldensis*. Reproductive structures (RS), the photobiont layers (PL) and lithocortex (LI) of lichens are recognizable before the staining step, which highlights the development of the hyphal penetration component (pHPC = pervasive hyphal penetration component; sHPC = sparse hyphal penetration component) beneath the rock surface (dotted white line). Microbial biofilm (MB). Sparse hyphae (SH) were sporadically observed beneath the epilithic biofilm. Scales: black bar. Further lithobiont profiles are reported in Supplementary material 1.

Figure 3. Lithobiont growth within the Botticino limestone (cross sections observed under RLM before –a,c,d,g- and after – b,d,f,h – staining by PAS): (a, b) epilithic microbial biofilm; (c, d) *Caloplaca ochracea*; (e, f) *Verrucaria nigrescens*; (g, h) *Bagliettoa baldensis*. Reproductive structures (RS), the photobiont layers (PL) and lithocortex (LI) of lichens are

recognizable before the staining step, which highlights the development of the hyphal penetration component (pHPC = pervasive hyphal penetration component; sHPC = sparse hyphal penetration component) beneath the rock surface (dotted white line). Microbial biofilm (MB). Sparse hyphae (SH) were sporadically observed beneath the epilithic biofilm. Scales: black bar. Further lithobiont profiles are reported in Supplementary material 1.

Figure 4. Anatomy of the lichen-rock interface as observed by RLM (a, d). Scales: black bar. and SEM in secondary electron (c, f, g, i, l) and BSE (BED-C: h, m; BED-S: b, e) modes (Scales: white bar). *Bagliettoa baldensis* (a-c) and *Porina linearis* (d-i) within Portland: (a, d) lithocortex and photobiont layers (LI-PL); (b) lichen-rock interface profile; (c) microcrystals at the lithocortex layer (LI), reproductive structures (RS); (e-f) appearance of the oolytic structure (OO) at the photobiont and deeper layers; (g-h) hyphae intermingled with microcrystals at the pHPC layers, associated to secondary porosity; (i) hyphae (H) within rock discontinuities at the sHPC layer; (l) *Bagliettoa baldensis* within Botticino: hyphae within rock discontinuities; (m) *Verrucaria nigrescens*-Botticino interface profile.

Figure 5. Water absorption capacity of Portland limestone colonized by microbial biofilm (P-a), epilithic (P-bC: *Caloplaca marina*) and endolithic (P-cP: *Porina linearis*; P-cB: *Bagliettoa baldensis*) lichens, before (white boxes) and after (grey boxes) removal/scraping procedures. Average absorption rate for each ten minutes interval between the different time points (left column) and total absorption at the different time points (right column). Time-points: 15 min (t_1), 30 min (t_2), 60 min (t_3), 120 min (t_4) and 240 min (t_5), with $t_0 = 0$ min. Boxes which do not share at least one letter are statistically different (Kruskal-Wallis and Mann-Whitney U Test; $p \leq 0.05$). Overview tables of statistical analyses are reported in Supplementary material 5.

Figure 6. Hybrid dynamic hardness (HDH_{robust}) of (P) Portland limestone, freshly broken (P-d), colonized by microbial biofilm (P-a), epilithic (P-bC: *Caloplaca marina*) and endolithic (P-cB: *Bagliettoa baldensis*; P-cP: *Porina linearis*) lichens, before (white boxes) and after (grey boxes) removal/scraping procedures, and (B) Botticino limestone, freshly broken (B-d), colonized by microbial biofilm (B-a), epilithic (B-bC: *Caloplaca ochracea*; B-bV: *Verrucaria nigrescens*) and endolithic (B-cB: *Bagliettoa baldensis*) lichens, before (white boxes) and after (grey boxes, REM) removal/scraping procedures. Boxes which do not share at least one letter are statistically different (Kruskal-Wallis and Mann-Whitney U Test; $p \leq 0.05$). Overview tables of statistical analyses are reported in Supplementary material 7.

Table 1. Profiles of the lithobiont-rock interfaces observed by RLM on cross-sections before and after staining by PAS. Data are reported as thickness ranges (μm) for the different characterized layers.

Lithology Lithobiont		Microbial biofilm		Epilithic thalline component (sensu Favero-Longo <i>et al.</i> , 2005)	Lichen-rock interface layers			
		Epilithic component	Sparse penetrating hyphae		Lithocortex (sensu Pinna <i>et al.</i> , 1998)	Endolithic photobiont layer (sensu Pinna <i>et al.</i> , 1998)	Hyphal penetration component [#] (sensu Favero-Longo <i>et al.</i> , 2005)	
							pervasive (pHPC)	sparse (sHPC)
		(MB)	(SH)	(TC)	(LI)	(PL)		
Portland								
Microbial biofilm	P-a	30-90	0-100	-	-	-	-	
<i>Caloplaca marina</i>	P-bC			100-300*	0-10**	70-130**	100-300	800-1000
<i>Porina linearis</i>	P-cP			-	0-30	70-150	300-1200	500-1700
<i>Bagliettoa baldensis</i>	P-cB			-	50-100	70-130	300-600	1500-2500
Botticino								
Microbial biofilm	B-a	30-50	0-100		-	-	-	-
<i>Caloplaca ochracea</i>	B-bC			100-300*	0-10**	100-200**	50-250	-
<i>Verrucaria nigrescens</i>	B-bV			150-250	-	-	600-800	0-200
<i>Bagliettoa baldensis</i>	B-cB			-	50-100	50-130	150-400	0-500

([#]) equivalent for endolithic species to the pseudomedulla layer (sensu Pinna *et al.*, 1998)

(*) the discontinuous epilithic thin thallus of *Caloplaca* species alternated with (**) an endolithic PL immersed beneath a crystalline film

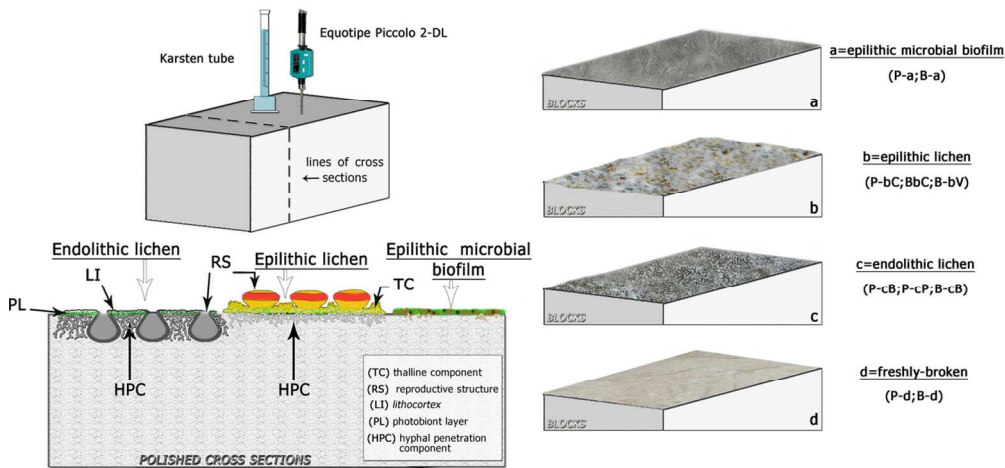


Figure 1. Lithobiont colonization types examined on Portland (P) and Botticino (B) limestones. Measurements of water absorption capacity and hardness were carried out by Karsten tube and Equotip on block surfaces, while the thickness and depth of the thalline (TC) and hyphal penetration (HPC) components (sensu Favero-Longo et al., 2005) of epilithic and endolithic lichens were examined on cross-sectioned profiles. Study cases are schematically summarized on the right picture side: (a) epilithic microbial biofilm on Portland (P-a) and Botticino (B-a); (b) epilithic lichens on Portland, *Caloplaca marina* (P-bC), and on Botticino, *Caloplaca ochracea* (B-bC) and *Verrucaria nigrescens* (B-bV); (c) endolithic lichens on Portland, *Porina linearis* (P-cP) and *Bagliettoa baldensis* (P-cB), and on Botticino, *Bagliettoa baldensis* (B-cB); d- freshly broken surfaces of Portland (P-d) and Botticino (B-d).

Figure 1
58x27mm (600 x 600 DPI)

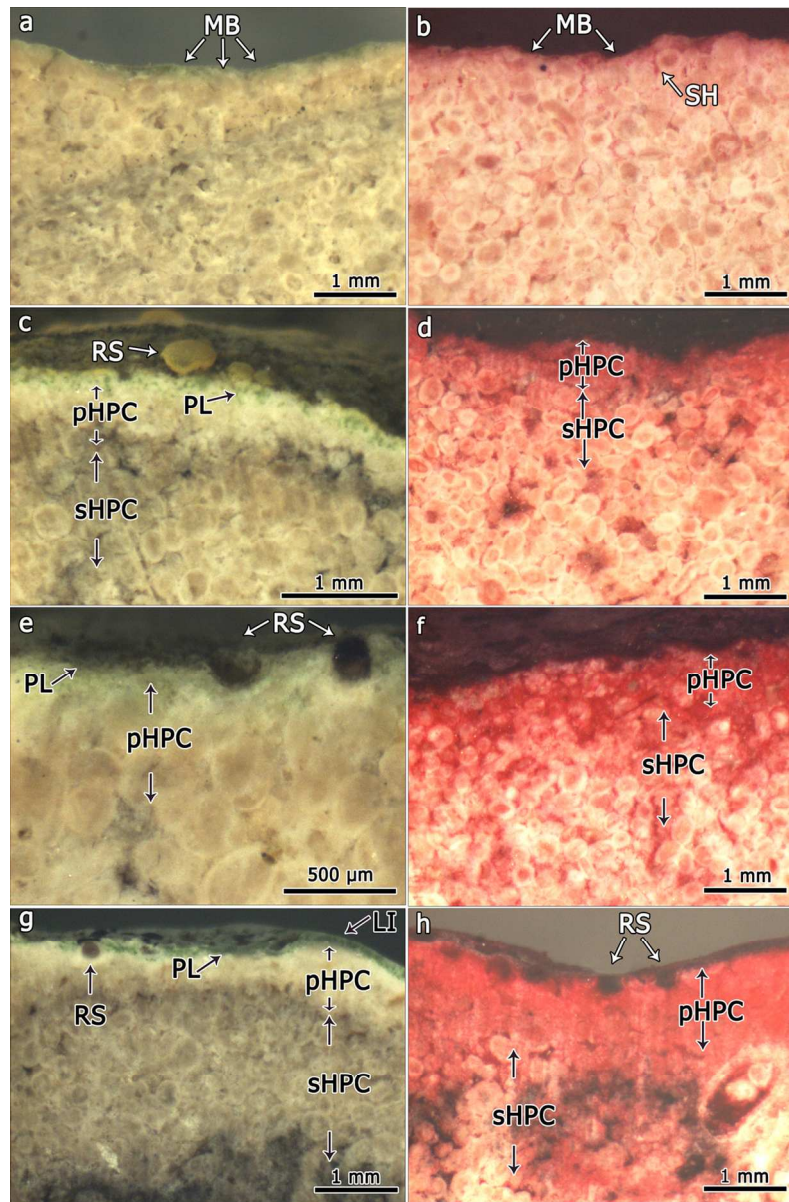


Figure 2. Lithobiont growth within the Portland limestone (cross sections observed under RLM before – a,c,d,g- and after – b,d,f,h – staining by PAS): (a, b) epilithic microbial biofilm; (c, d) *Caloplaca marina*; (e, f) *Porina linearis*; (g, h) *Bagliettoa baldensis*. Reproductive structures (RS), the photobiont layers (PL) and lithocortex (LI) of lichens are recognizable before the staining step, which highlights the development of the hyphal penetration component (pHPC = pervasive hyphal penetration component; sHPC = sparse hyphal penetration component) beneath the rock surface (dotted white line). Microbial biofilm (MB). Sparse hyphae (SH) were sporadically observed beneath the epilithic biofilm. Scales: black bar. Further lithobiont profiles are reported in Supplementary material 1.

Figure 2

117x179mm (300 x 300 DPI)

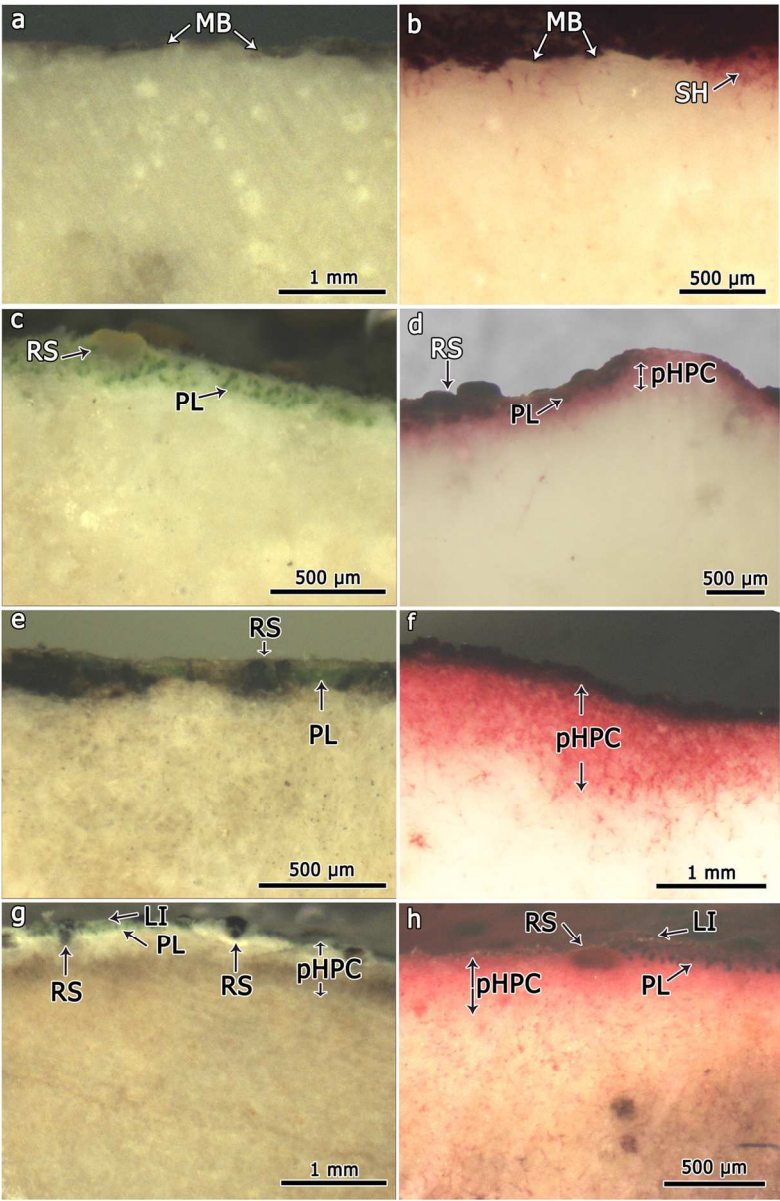


Figure 3. Lithobiont growth within the Botticino limestone (cross sections observed under RLM before – a,c,d,g- and after – b,d,f,h – staining by PAS): (a, b) epilithic microbial biofilm; (c, d) *Caloplaca ochracea*; (e, f) *Verrucaria nigrescens*; (g, h) *Bagliettoa baldensis*. Reproductive structures (RS), the photobiont layers (PL) and lithocortex (LI) of lichens are recognizable before the staining step, which highlights the development of the hyphal penetration component (pHPC = pervasive hyphal penetration component; SHPC = sparse hyphal penetration component) beneath the rock surface (dotted white line). Microbial biofilm (MB). Sparse hyphae (SH) were sporadically observed beneath the epilithic biofilm. Scales: black bar. Further lithobiont profiles are reported in Supplementary material 1.

Figure 3

119x184mm (300 x 300 DPI)

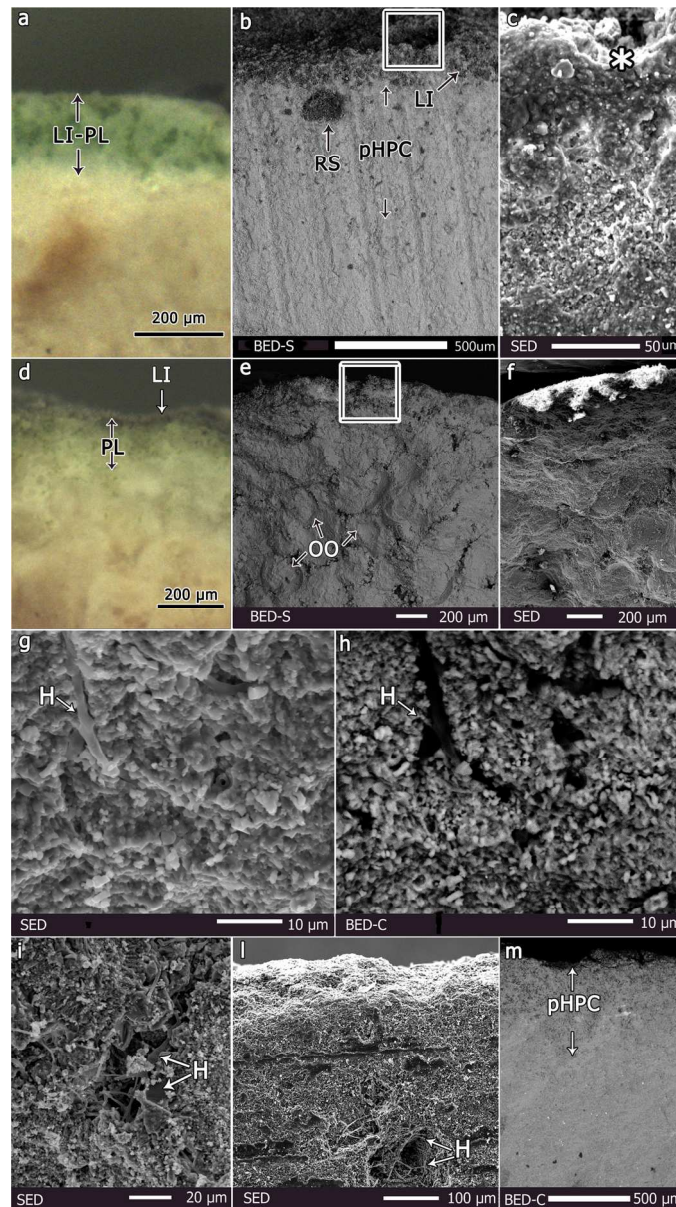


Figure 4. Anatomy of the lichen-rock interface as observed by RLM (a, d). Scales: black bar. and SEM in secondary electron (c, f, g, i, l) and BSE (BED-C: h, m; BED-S: b, e) modes (Scales: white bar). *Bagliettoa baldensis* (a-c) and *Porina linearis* (d-i) within Portland: (a, d) lithocortex and photobiont layers (LI-PL); (b) lichen-rock interface profile; (c) microcrystals at the lithocortex layer (LI), reproductive structures (RS); (e-f) appearance of the oolytic structure (OO) at the photobiont and deeper layers; (g-h) hyphae intermingled with microcrystals at the pHPC layers, associated to secondary porosity; (i) hyphae (H) within rock discontinuities at the sHPC layer; (l) *Bagliettoa baldensis* within Botticino: hyphae within rock discontinuities; (m) *Verrucaria nigrescens*-Botticino interface profile.

Figure 4

117x209mm (300 x 300 DPI)

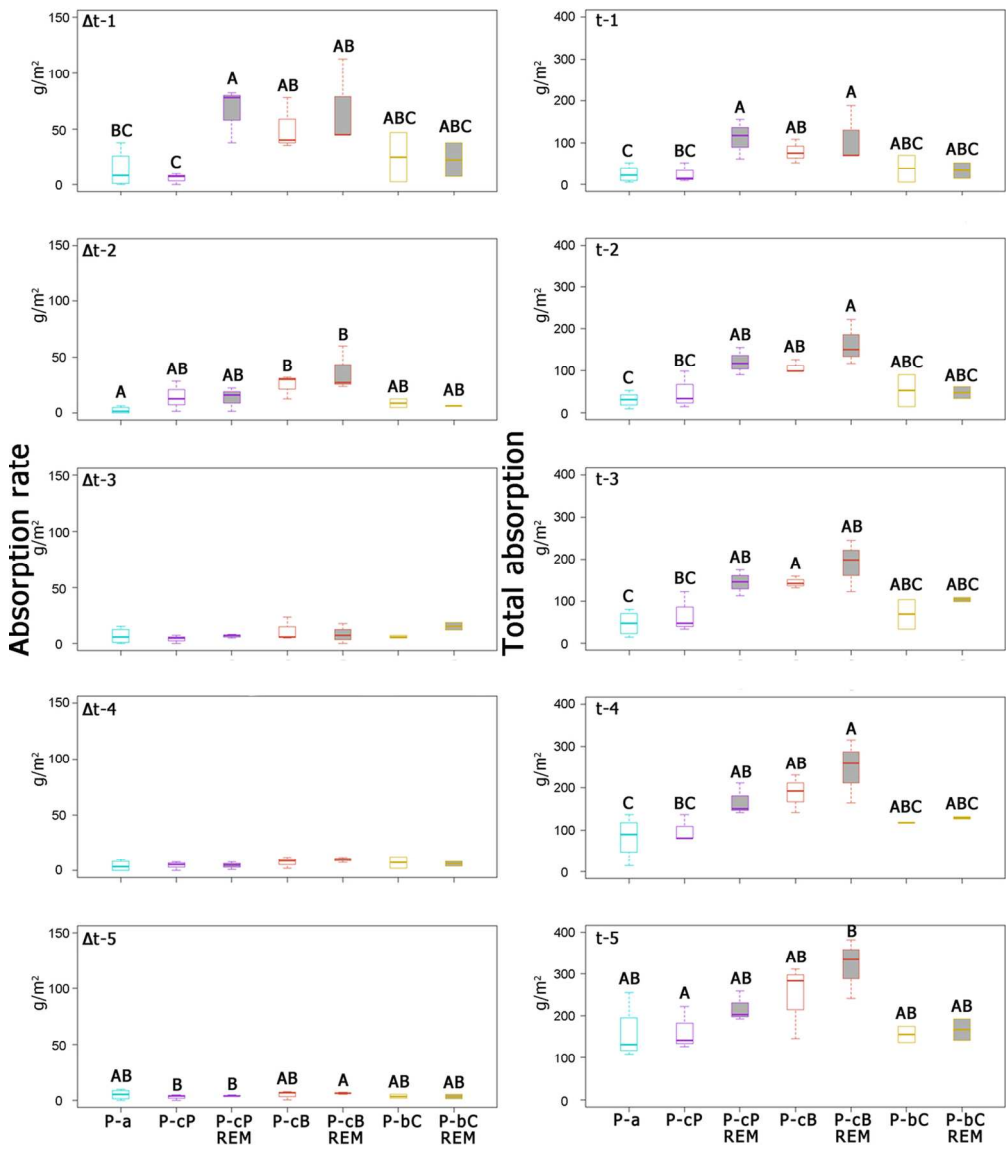


Figure 5. Water absorption capacity of Portland limestone colonized by microbial biofilm (P-a), epilithic (P-bC: *Caloplaca marina*) and endolithic (P-cP: *Porina linearis*; P-cB: *Bagliettoa baldensis*) lichens, before (white boxes) and after (grey boxes) removal/scraping procedures. Average absorption rate for each ten minutes interval between the different time points (left column) and total absorption at the different time points (right column). Time-points: 15 min (t1), 30 min (t2), 60 min (t3), 120 min (t4) and 240 min (t5), with t0 = 0 min. Boxes which do not share at least one letter are statistically different (Kruskal-Wallis and Mann-Whitney U Test; $p \leq 0.05$). Overview tables of statistical analyses are reported in Supplementary material 5.

Figure 5
119x141mm (300 x 300 DPI)

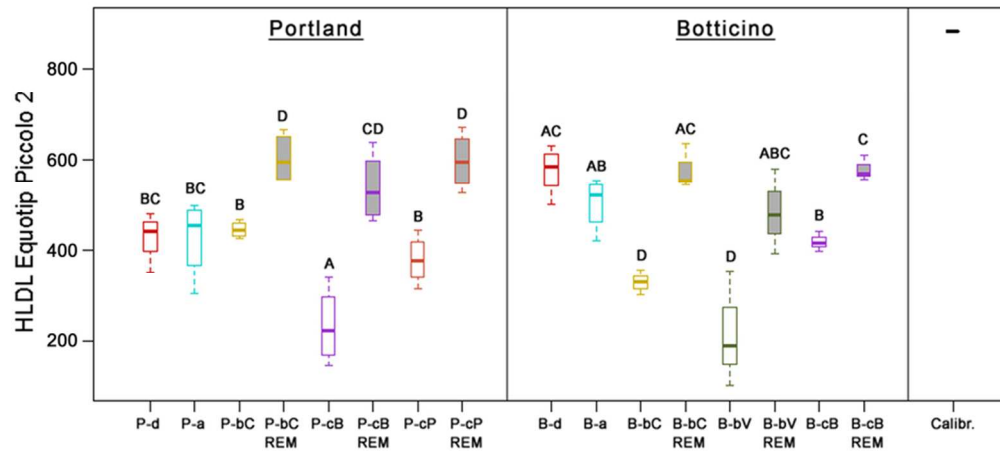


Figure 6. Hybrid dynamic hardness (HDHrobust) of (P) Portland limestone, freshly broken (P-d), colonized by microbial biofilm (P-a), epilithic (P-bC: *Caloplaca marina*) and endolithic (P-cB: *Bagliettoa baldensis*; P-cP: *Porina linearis*) lichens, before (white boxes) and after (grey boxes) removal/scraping procedures, and (B) Botticino limestone, freshly broken (B-d), colonized by microbial biofilm (B-a), epilithic (B-bC: *Caloplaca ochracea*; B-bV: *Verrucaria nigrescens*) and endolithic (B-cB: *Bagliettoa baldensis*) lichens, before (white boxes) and after (grey boxes, REM) removal/scraping procedures. Boxes which do not share at least one letter are statistically different (Kruskal-Wallis and Mann-Whitney U Test; $p \leq 0.05$). Overview tables of statistical analyses are reported in Supplementary material 7.

Figure 6
80x36mm (300 x 300 DPI)

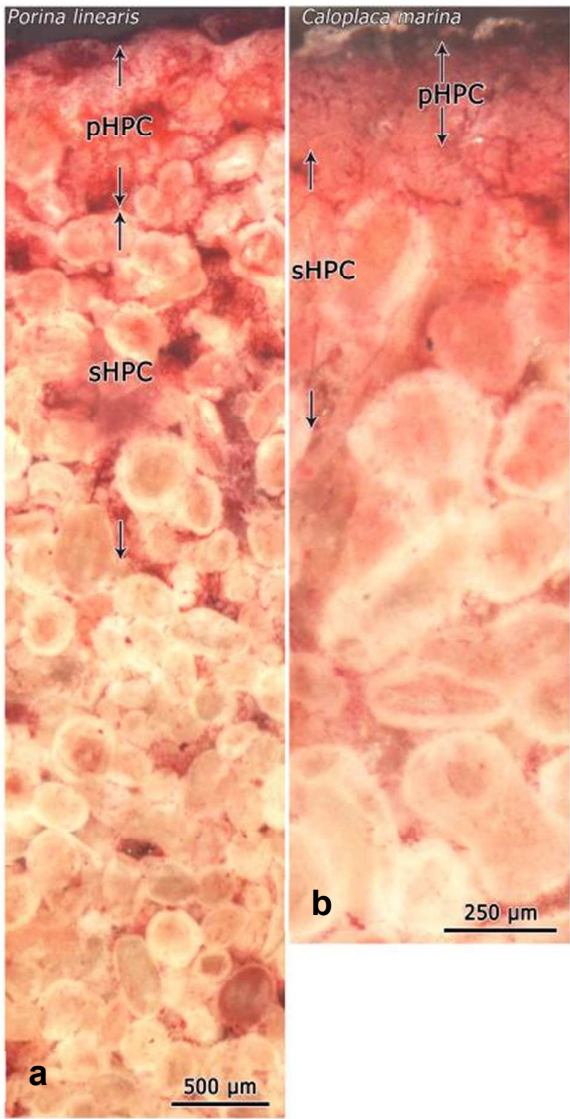
The influence of structural organization on the impact of epilithic and endolithic lichens on limestone weathering

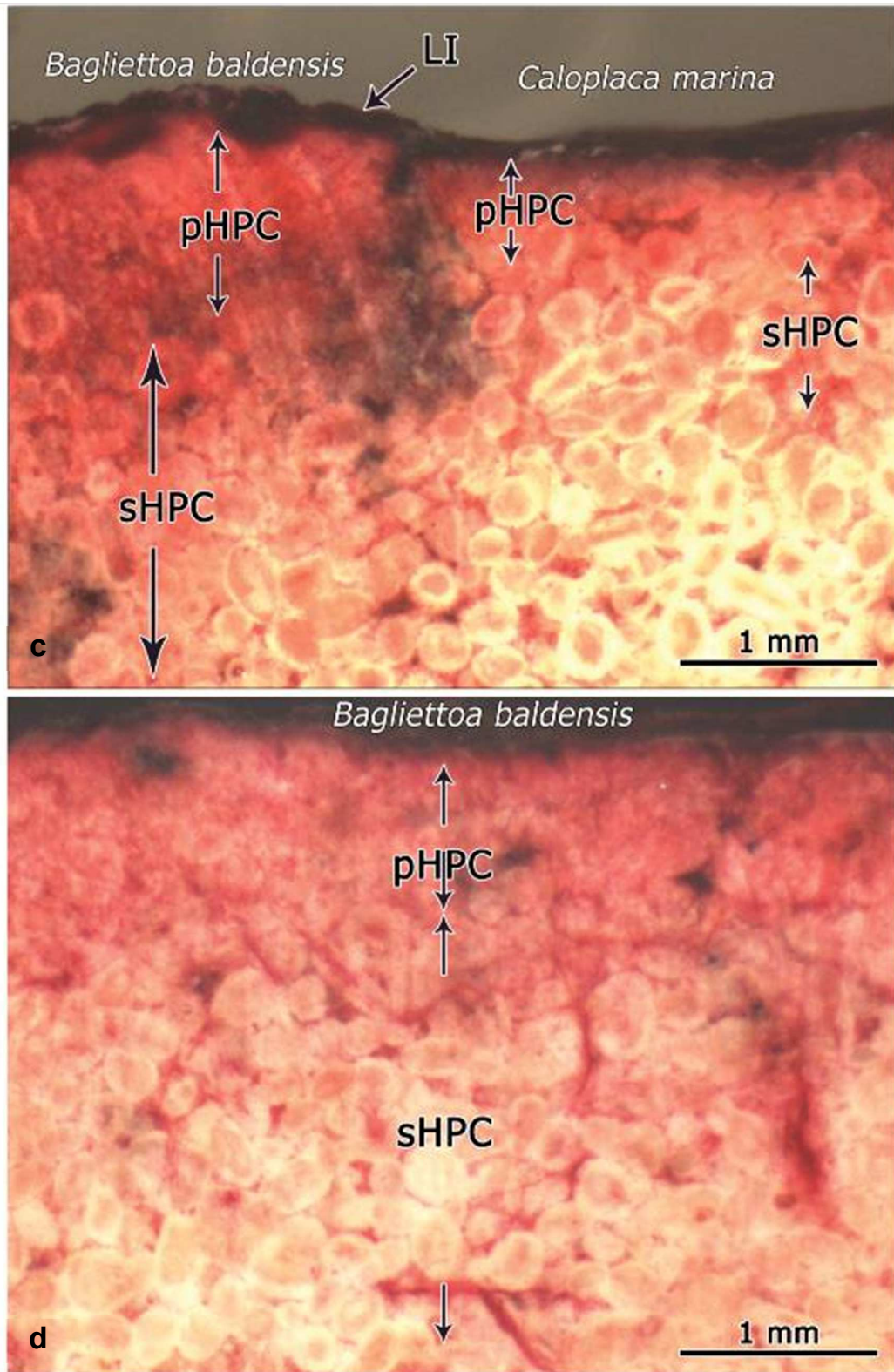
Morando M.¹, Wilhelm K.², Matteucci E.¹, Martire L.³, Piervittori R.¹, Viles H.², Favero-Longo S.E.^{1,*}

1 - University of Torino, Department of Life Sciences and Systems Biology, Viale Mattioli 25, 10125, Torino, Italy
2 - Oxford Rock Breakdown Laboratory (OxRBL), School of Geography and the Environment, University of Oxford, Oxford, UK
3 - University of Torino, Department of Earth Sciences, Via Valperga Caluso 35, 10125, Torino, Italy

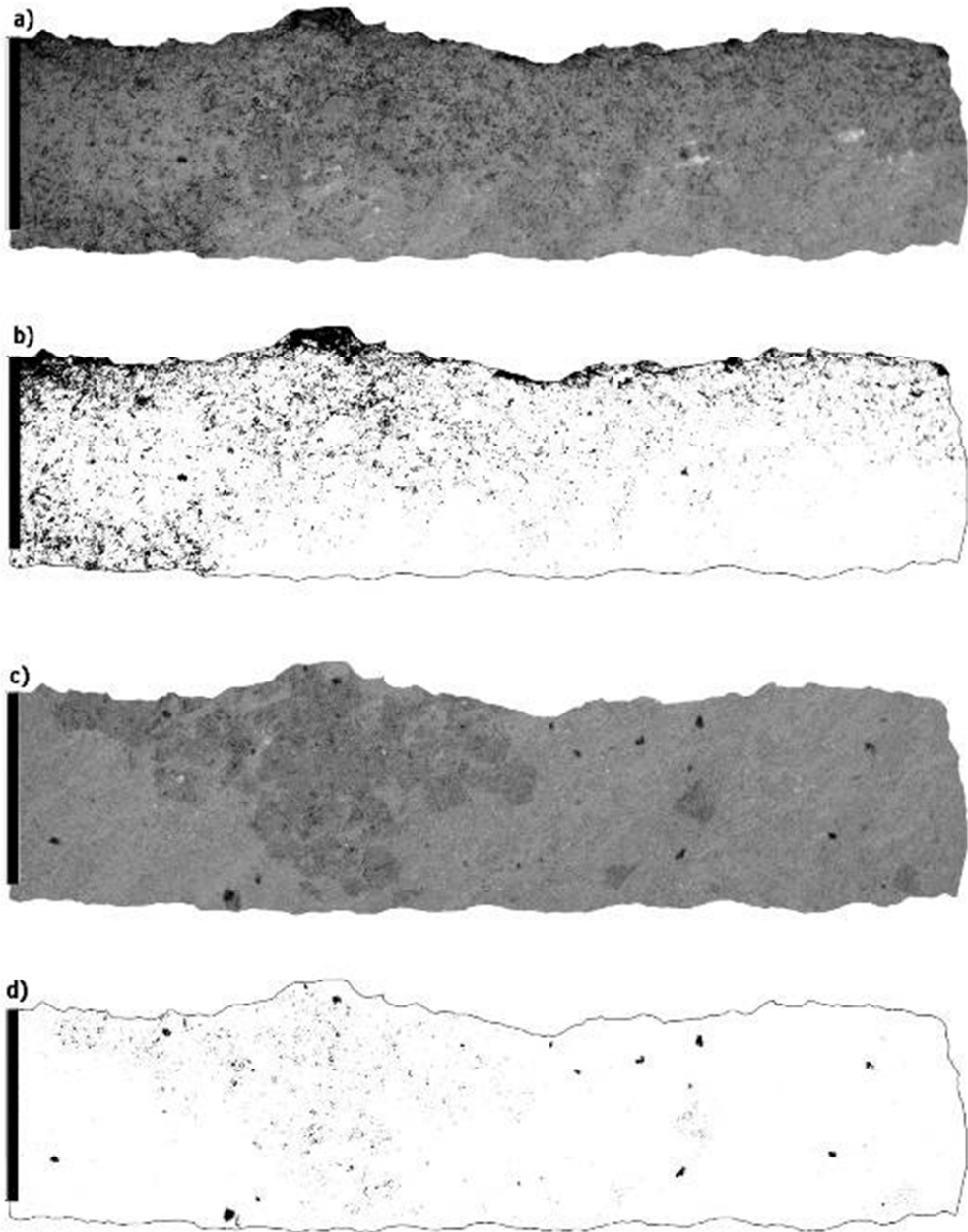
Supplementary materials

Supplementary material 1. Profiles on Portland limestone (cross sections observed under RLM after staining by PAS) colonized by *Porina linearis* (a), *Caloplaca marina* (b), *Bagliettoa baldensis* and *Caloplaca marina* (c), *Bagliettoa baldensis* (d). Hyphal penetration component (pHPC = pervasive hyphal penetration component; sHPC = sparse hyphal penetration component); lithocortex (LI). Scales: black bars.

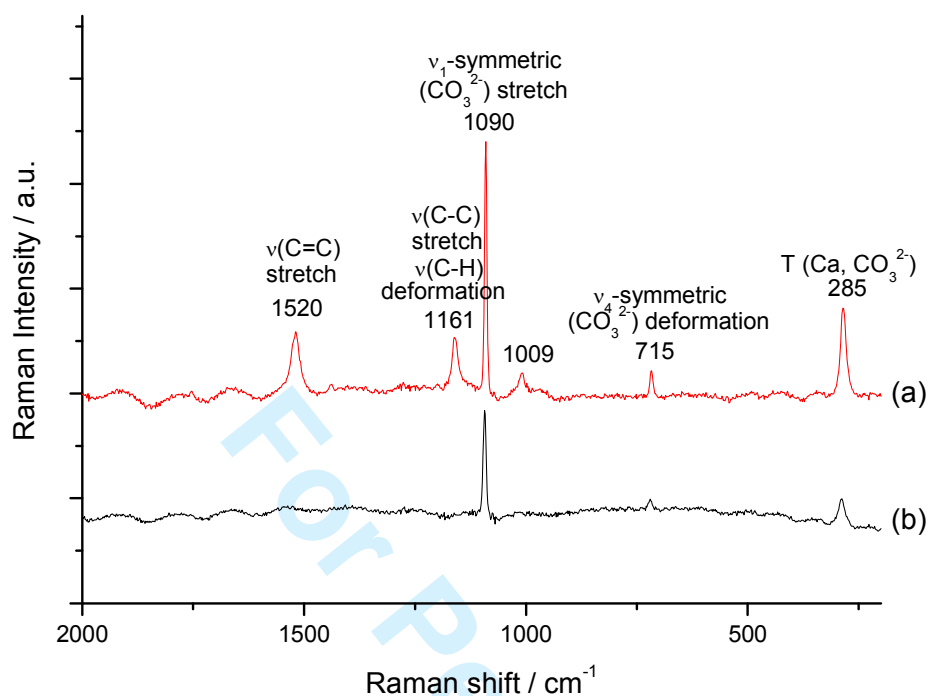




Supplementary material 2. BSE imaging (a-c) and related image analyses of porosity s.l. (black coloured, visualized by imageJ) of *V. nigrescens* on Botticino: (a-b) profile of the lichen-rock interface from the surface down to approx. 500 µm within the rock; (c-d) profile of the uncolonized layer from approx. 500 µm to 1 mm.

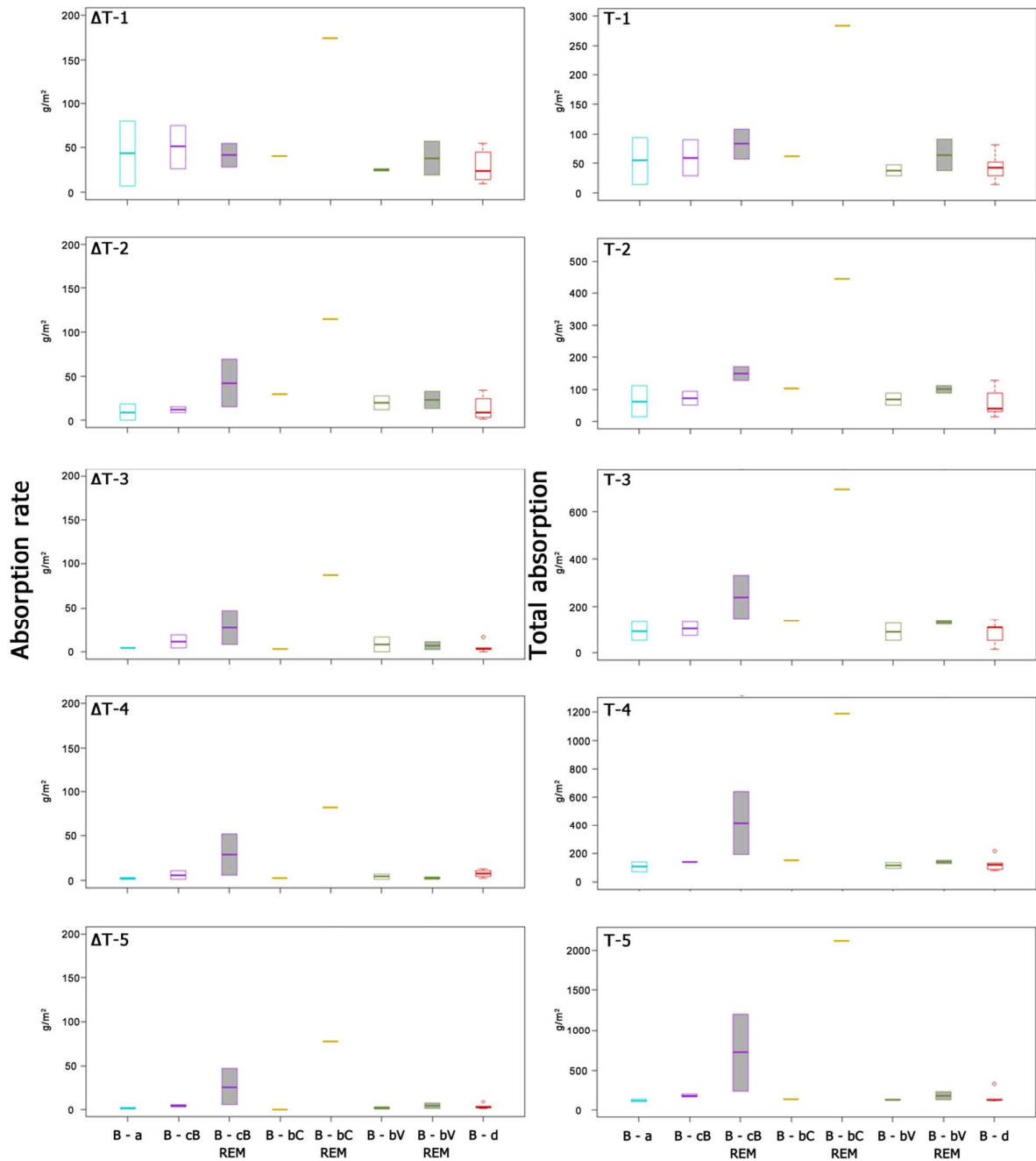


Supplementary material 3. Micro-Raman spectra collected (a) at the LI layer of *Bagliettoa baldensis* and (b) at a deeper uncolonized level.



Supplementary material 4

Botticino limestone: Karsten tube absorption (sample codes as in Figure 6). Overview tables of statistical analyses are reported in Supplementary material 5.



Supplementary material 5

Statistics on water absorption: Kruskal-Wallis and Mann-Whitney U Test ($p \leq 0.05$ as significantly different, *).

Portland limestone**Total absorption**

t1	P-a	P-cP	P-cP REM	P-cB	P-cB REM	P-bC	P-bC REM
P-a n=4	1.000						
P-cP n=3	0.853	1.000					
P-cP REM n=3	0.034*	0.046*	1.000				
P-cB n=3	0.050*	0.072	0.275	1.000			
P-cB REM n=3	0.032*	0.043*	0.825	0.825	1.000		
P-bC n=2	0.814	1.000	0.248	0.248	0.197	1.000	
P-bC REM n=2	0.634	0.739	0.083	0.139	0.076	1.000	1.000
t2	P-a	P-cP	P-cP REM	P-cB	P-cB REM	P-bC	P-bC REM
P-a n=4	1.000						
P-cP n=3	0.853	1.000					
P-cP REM n=3	0.032*	0.127	1.000				
P-cB n=3	0.031*	0.105	0.825	1.000			
P-cB REM n=3	0.032*	0.050*	0.376	0.121	1.000		
P-bC n=2	0.812	0.767	0.139	0.076	0.083	1.000	
P-bC REM n=2	0.325	0.767	0.083	0.076	0.083	1.000	1.000
t3	P-a	P-cP	P-cP REM	P-cB	P-cB REM	P-bC	P-bC REM
P-a n=4	1.000						
P-cP n=3	0.593	1.000					
P-cP REM n=3	0.034*	0.127	1.000				
P-cB n=3	0.034*	0.050*	0.827	1.000			
P-cB REM n=3	0.034*	0.077	0.275	0.513	1.000		
P-bC n=2	0.481	0.767	0.083	0.083	0.083	1.000	
P-bC REM n=2	0.064	0.564	0.139	0.083	0.083	0.221	1.000

t4	P-a	P-cP	P-cP REM	P-cB	P-cB REM	P-bC	P-bC REM
P-a n=4	1.000						
P-cP n=3	0.853	1.000					
P-cP REM n=3	0.050*	0.072	1.000				
P-cB n=3	0.050*	0.072	0.658	1.000			
P-cB REM n=3	0.034*	0.046*	0.127	0.275	1.000		
P-bC n=2	0.348	0.543	0.076	0.076	0.076	1.000	
P-bC REM n=2	0.348	0.543	0.076	0.076	0.076	0.083	1.000
t5	P-a	P-cP	P-cP REM	P-cB	P-cB REM	P-bC	P-bC REM
P-a n=4	1.000						
P-cP n=3	0.719	1.000					
P-cP REM n=3	0.157	0.275	1.000				
P-cB n=3	0.077	0.127	0.513	1.000			
P-cB REM n=3	0.077	0.050*	0.127	0.275	1.000		
P-bC n=2	0.481	0.767	0.083	0.248	0.083	1.000	
P-bC REM n=2	0.481	0.767	0.139	0.248	0.083	0.683	1.000
Absorption rate							
Δ -t1	P-a	P-cP	P-cP REM	P-cB	P-cB REM	P-bC	P-bC REM
P-a n=4	1.000						
P-cP n=3	1.000	1.000					
P-cP REM n=3	0.046*	0.043*	1.000				
P-cB n=3	0.064	0.043*	0.456	1.000			
P-cB REM n=3	0.064	0.043*	0.814	0.796	1.000		
P-bC n=2	0.623	0.761	0.236	0.554	0.554	1.000	
P-bC REM n=2	0.333	0.197	0.128	0.197	0.197	1.000	1.000
Δ -t2	P-a	P-cP	P-cP REM	P-cB	P-cB REM	P-bC	P-bC REM
P-a n=4	1.000						
P-cP n=3	0.237	1.000					
P-cP REM n=3	0.167	1.000	1.000				
P-cB n=3	0.040*	0.346	0.261	1.000			
P-cB REM n=3	0.028	0.184	0.105	0.487	1.000		
P-bC n=2	0.576	0.543	0.361	0.128	0.083	1.000	
P-bC REM n=2	0.114	1.000	0.543	0.182	0.076	0.317	1.000

Δ -t3	P-a	P-cP	P-cP REM	P-cB	P-cB REM	P-bC	P-bC REM
P-a n=4	1.000						
P-cP n=3	0.554	1.000					
P-cP REM n=3	1.000	0.456	1.000				
P-cB n=3	0.708	0.346	0.637	1.000			
P-cB REM n=3	0.708	0.346	0.637	1.000	1.000		
P-bC n=2	0.803	0.739	0.739	0.543	0.543	1.000	
P-bC REM n=2	0.333	0.128	0.197	0.543	0.543	0.221	1.000
Δ -t4	P-a	P-cP	P-cP REM	P-cB	P-cB REM	P-bC	P-bC REM
P-a n=4	1.000						
P-cP n=3	0.683	1.000					
P-cP REM n=3	0.683	0.456	1.000				
P-cB n=3	0.683	1.000	0.456	1.000			
P-cB REM n=3	0.180	0.317	0.114	0.317	1.000		
P-bC n=2	1.000	0.739	0.739	0.739	0.221	1.000	
P-bC REM n=2	1.000	0.739	0.739	0.739	0.221	1.000	1.000
Δ -t5	P-a	P-cP	P-cP REM	P-cB	P-cB REM	P-bC	P-bC REM
P-a n=4	1.000						
P-cP n=3	0.180	1.000					
P-cP REM n=3	0.180	1.000	1.000				
P-cB n=3	0.683	0.114	0.114	1.000			
P-cB REM n=3	0.180	0.025	0.025	0.317	1.000		
P-bC n=2	1.000	0.221	0.221	0.739	0.221	1.000	
P-bC REM n=2	1.000	0.221	0.221	0.739	0.221	1.000	1.000

Botticino limestone

Total absorption

t-1	B-a	B-cB	B-cB REM	B-bC	B-bC REM	B-bV	B-bV REM	B-d
B-a n=2	1.000							
B-cB n=2	0.683	1.000						
B-cB REM n=2	0.439	0.439	1.000					
B-bC n=1	1.000	1.000	0.480	1.000				
B-bC REM n=1	0.221	0.221	0.221	0.317	1.000			
B-bV n=2	1.000	0.683	0.121	0.221	0.221	1.000		
B-bV REM n=2	0.683	0.683	0.439	1.000	0.221	0.439	1.000	
B-d n=5	0.845	0.558	0.121	0.380	0.143	1.000	0.329	1.000

t-2	B-a	B-cB	B-cB REM	B-bC	B-bC REM	B-bV	B-bV REM	B-d
B-a n=2	1.000							
B-cB n=2	1.000	1.000						
B-cB REM n=2	0.121	0.121	1.000					
B-bC n=1	1.000	0.221	0.221	1.000				
B-bC REM n=1	0.221	0.221	0.221	0.317	1.000			
B-bV n=2	1.000	1.000	0.121	0.221	0.221	1.000		
B-bV REM n=2	0.683	0.221	0.121	1.000	0.221	0.221	1.000	
B-d n=5	0.845	0.558	0.079	0.380	0.143	0.558	0.329	1.000
t-3	B-a	B-cB	B-cB REM	B-bC	B-bC REM	B-bV	B-bV REM	B-d
B-a n=2	1.000							
B-cB n=2	0.683	1.000						
B-cB REM n=2	0.121	0.121	1.000					
B-bC n=1	0.221	0.221	0.221	1.000				
B-bC REM n=1	0.221	0.221	0.221	0.317	1.000			
B-bV n=2	1.000	0.683	0.121	0.221	0.221	1.000		
B-bV REM n=2	0.439	0.439	0.121	0.480	0.221	0.439	1.000	
B-d n=5	0.844	0.696	0.051	0.228	0.137	0.844	0.167	1.000
t-4	B-a	B-cB	B-cB REM	B-bC	B-bC REM	B-bV	B-bV REM	B-d
B-a n=2	1.000							
B-cB n=2	0.317	1.000						
B-cB REM n=2	0.121	0.102	1.000					
B-bC n=1	0.221	0.157	0.221	1.000				
B-bC REM n=1	0.221	0.157	0.221	0.317	1.000			
B-bV n=2	0.683	0.317	0.121	0.221	0.221	1.000		
B-bV REM n=2	0.439	1.000	0.121	0.480	0.221	0.439	1.000	
B-d n=5	0.699	0.241	0.121	0.380	0.143	0.845	0.329	1.000
t-5	B-a	B-cB	B-cB REM	B-bC	B-bC REM	B-bV	B-bV REM	B-d
B-a n=2	1.000							
B-cB n=2	0.121	1.000						
B-cB REM n=2	0.121	0.121	1.000					
B-bC n=1	0.480	0.221	0.221	1.000				
B-bC REM n=1	0.221	0.221	0.221	0.317	1.000			
B-bV n=2	0.683	0.121	0.121	0.480	0.221	1.000		
B-bV REM n=2	0.439	1.000	0.121	1.000	0.221	0.683	1.000	
B-d n=5	0.554	0.241	0.118	0.546	0.137	0.839	0.688	1.000

Absorption rate

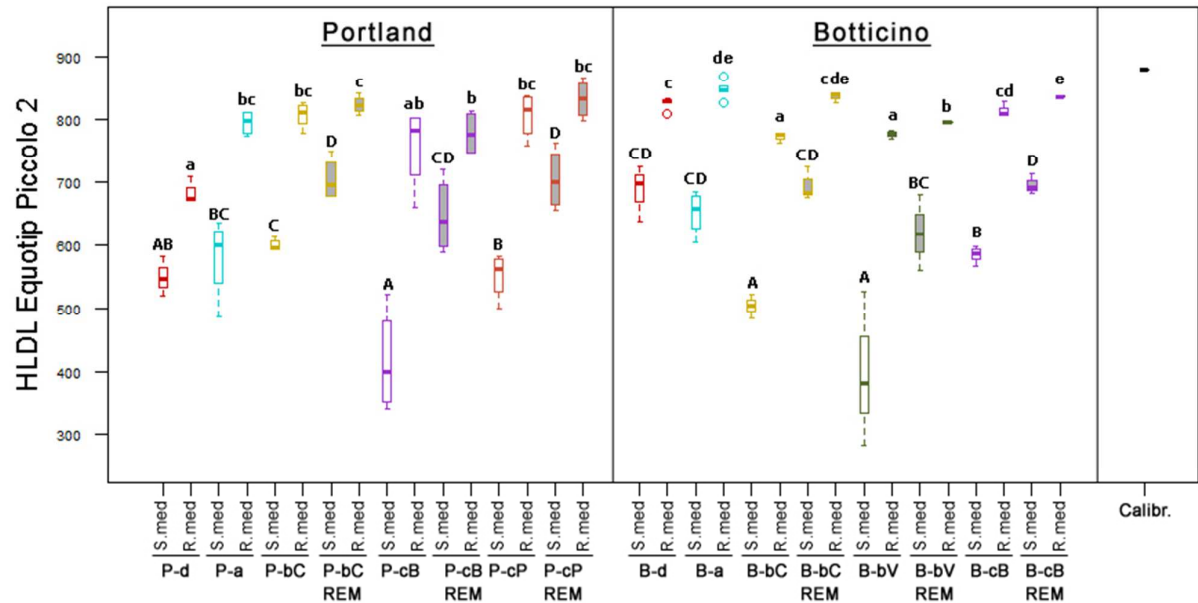
Δ -t1	B-a	B-cB	B-cB REM	B-bC	B-bC REM	B-bV	B-bV REM	B-d
B-a n=2	1.000							
B-cB n=2	0.683	1.000						
B-cB REM n=2	1.000	0.683	1.000					
B-bC n=1	1.000	1.000	1.000	1.000				
B-bC REM n=1	0.221	0.221	0.221	0.317	1.000			
B-bV n=2	1.000	0.221	0.221	0.221	0.221	1.000		
B-bV REM n=2	1.000	0.439	1.000	1.000	0.221	0.683	1.000	
B-d n=5	0.688	0.241	0.324	0.546	0.137	0.844	0.324	1.000
Δ -t2	B-a	B-cB	B-cB REM	B-bC	B-bC REM	B-bV	B-bV REM	B-d
B-a n=2	1.000							
B-cB n=2	0.683	1.000						
B-cB REM n=2	0.221	0.221	1.000					
B-bC n=1	0.221	0.221	1.000	1.000				
B-bC REM n=1	0.221	0.221	0.221	0.317	1.000			
B-bV n=2	0.439	0.683	0.439	0.480	0.221	1.000		
B-bV REM n=2	0.439	0.683	0.439	0.480	0.221	1.000	1.000	
B-d n=5	0.685	0.842	0.237	0.343	0.132	0.539	0.539	1.000
Δ -t3	B-a	B-cB	B-cB REM	B-bC	B-bC REM	B-bV	B-bV REM	B-d
B-a n=2	1.000							
B-cB n=2	0.317	1.000						
B-cB REM n=2	0.102	0.439	1.000					
B-bC n=1	1.000	0.480	0.221	1.000				
B-bC REM n=1	0.157	0.221	0.221	0.317	1.000			
B-bV n=2	0.317	1.000	0.439	0.480	0.221	1.000		
B-bV REM n=2	0.317	0.683	0.221	0.480	0.221	0.683	1.000	
B-d n=5	0.527	0.462	0.087	0.655	0.083	0.462	0.629	1.000
Δ -t4	B-a	B-cB	B-cB REM	B-bC	B-bC REM	B-bV	B-bV REM	B-d
B-a n=2	1.000							
B-cB n=2	0.317	1.000						
B-cB REM n=2	0.102	0.221	1.000					
B-bC n=1	1.000	0.480	0.221	1.000				
B-bC REM n=1	0.157	0.221	0.221	0.317	1.000			
B-bV n=2	0.317	1.000	0.221	0.480	0.221	1.000		
B-bV REM n=2	1.000	0.317	0.102	1.000	0.157	0.317	1.000	
B-d n=5	0.180	0.823	0.130	0.317	0.114	0.823	0.180	1.000

Δ -t5	B-a	B-cB	B-cB REM	B-bC	B-bC REM	B-bV	B-bV REM	B-d
B-a n=2	1.000							
B-cB n=2	0.317	1.000						
B-cB REM n=2	0.102	0.221	1.000					
B-bC n=1	1.000	0.480	0.221	1.000				
B-bC REM n=1	0.157	0.221	0.221	0.317	1.000			
B-bV n=2	1.000	0.317	0.102	1000	0.157	1.000		
B-bV REM n=2	0.317	1.000	0.221	0.480	0.221	0.317	1.000	
B-d n=5	0.527	0.462	0.052	0.655	0.083	0.527	0.462	1.000

For Peer Review

Supplementary material 6

HLDL (hardness values obtained with the DL probe), single impact method (SIM), median (S_{med}) and median of the three highest values in each of the three repeated impact method (RIM) datasets of 20 readings (R_{med}) on (P) Portland limestone, freshly broken (P-d), colonized by microbial biofilm (P-a), epilithic (P-bC: *Caloplaca marina*) and endolithic (P-cP: *Porina linearis*; P-cB: *Bagliettoa baldensis*) lichens, before (white boxes) and after (grey boxes) removal/scraping procedures, and (B) Botticino limestone, freshly broken (B-d), colonized by microbial biofilm (B-a), epilithic (B-bC: *Caloplaca ochracea*; B-bV: *Verrucaria nigrescens*) and endolithic (B-cB: *Bagliettoa baldensis*) lichens, before (white boxes) and after (grey boxes, REM) removal/scraping procedures. Boxes which do not share at least one letter are statistically different (Kruskal-Wallis and Mann-Whitney U Test; $p < 0.05$).



Overview tables of statistical analyses are reported in Supplementary material 7.

Supplementary material 7.

Statistics on Hybrid dynamic hardness (HDH_{robust}) and HLDL hardness (S.med; R.med) on Portland limestone and Botticino limenstone: Kruskal-Wallis and Mann-Whitney U Test (p≤0.05 as significantly different, *).

Portland limestone

HDH _{DL robust}	P-d	P-a	P-bc	P-bC-REM	P-cB	P-cB-REM	P-cP	P-cP-REM
P-d n=3	1.000							
P-a n=4	1.000	1.000						
P-bc n=4	1.000	0.773	1.000					
P-bC-REM n=4	0.034*	0.021*	0.021*	1.000				
P-cB n=4	0.034*	0.043*	0.021*	0.021*	1.000			
P-cB-REM n=4	0.077	0.149	0.043*	0.309	0.021*	1.000		
P-cP n=4	0.480	0.386	0.083	0.021*	0.043*	0.021*	1.000	
P-cP-REM n=4	0.034*	0.021*	0.021*	1.000	0.021*	0.248	0.021*	1.000

HLDL SIM	P-d SIM	P-a SIM	P-bC SIM	P-bC SIM REM	P-cB SIM	P-cB SIM REM	P-cP SIM	P-cP SIM REM
P-d SIM n=3	1.000							
P-a SIM n=4	0.289	1.000						
P-bC SIM n=4	0.032*	0.772	1.000					
P-bC SIM REM n=4	0.032*	0.020*	0.019*	1.000				
P-cB SIM n=4	0.077	0.043*	0.020*	0.020*	1.000			
P-cB SIM REM n=4	0.034*	0.386	0.384	0.146	0.021*	1.000		
P-cP SIM n=4	1.000	0.248	0.020*	0.020*	0.043*	0.021*	1.000	
P-cP SIM REM n=4	0.034*	0.021*	0.020*	0.772	0.021*	0.149	0.021*	1.000

HLDL RIM	P-d RIM	P-a RIM	P-bC RIM	P-bC RIM REM	P-cB RIM	P-cB RIM REM	P-cP RIM	P-cP RIM REM
P-d RIM n=3	1.000							
P-a RIM n=4	0.032*	1.000						
P-bC RIM n=4	0.034*	0.384	1.000					
P-bC RIM REM n=4	0.034*	0.081	0.309	1.000				
P-cB RIM n=4	0.289	0.245	0.083	0.021*	1.000			
P-cB RIM REM n=4	0.034*	0.561	0.149	0.043*	0.564	1.000		
P-cP RIM n=4	0.034*	0.561	0.773	0.564	0.386	0.248	1.000	
P-cP RIM REM n=4	0.034*	0.081	0.386	0.773	0.083	0.083	0.248	1.000

Botticino limestone

HDH_{DL} robust	B-a	B-d	B-cB	B-bC	B-bV	B-cB REM	B-bC REM	B-bV REM
B-a n=5	1.000							
B-d n=5	0.117	1.000						
B-cB n=3	0.053	0.025*	1.000					
B-bC n=3	0.025*	0.025*	0.050*	1.000				
B-bV n=3	0.025*	0.025*	0.050*	0.275	1.000			
B-cB REM n=3	0.025*	0.881	0.050*	0.050*	0.050*	1.000		
B-bC REM n=3	0.072	0.655	0.050*	0.050*	0.050*	0.513	1.000	
B-bV REM n=3	0.881	0.101	0.513	0.050*	0.050*	0.275	0.275	1.000

HLDL SIM	B-d SIM	B-a SIM	B-bC SIM	B-bC SIM REM	B-bV SIM	B-bV SIM REM	B-cB SIM	B-cB SIM REM
B-d SIM n=5	1.000							
B-a SIM n=5	0.117	1.000						
B-bC SIM n=3	0.025*	0.025*	1.000					
B-bC SIM REM n=3	0.764	0.180	0.050*	1.000				
B-bV SIM n=3	0.025*	0.025*	0.513	0.050*	1.000			
B-bV SIM REM n=3	0.101	0.456	0.050*	0.127	0.050*	1.000		
B-cB SIM n=3	0.025*	0.025*	0.050*	0.050*	0.050*	0.513	1.000	
B-cB SIM REM n=3	0.881	0.053	0.050*	0.658	0.050*	0.050*	0.050*	1.000
HLDL RIM	B-d RIM	B-a RIM	B-bC RIM	B-bC RIM REM	B-bV RIM	B-bV RIM REM	B-cB RIM	B-cB RIM REM
B-d RIM n=5	1.000							
B-a RIM n=5	0.047*	1.000						
B-bC RIM n=3	0.025*	0.025*	1.000					
B-bC RIM REM n=3	0.230	0.101	0.050*	1.000				
B-bV RIM n=3	0.025*	0.025*	0.513	0.050*	1.000			
B-bV RIM REM n=3	0.025*	0.025*	0.050*	0.050*	0.050*	1.000		
B-cB RIM n=3	0.101	0.053	0.050*	0.127	0.050*	0.050*	1.000	
B-cB RIM REM n=3	0.036*	0.180	0.050*	0.513	0.050*	0.050*	0.050*	1.000

The influence of structural organization ~~on the impact~~ of epilithic and endolithic lichens on limestone weathering

Morando M.¹, Wilhelm K.², Matteucci E.¹, Martire L.³, Piervittori R.¹, Viles H.A.², Favero-Longo S.E.^{1,*}

1 - University of Torino, Department of Life Sciences and Systems Biology, Viale Mattioli 25, 10125, Torino, Italy

2 - Oxford Rock Breakdown Laboratory (OxRBL), School of Geography and the Environment, University of Oxford, Oxford, UK

3 - University of Torino, Department of Earth Sciences, Via Valperga Caluso 35, 10125, Torino, Italy

*Corresponding author:

Sergio Enrico Favero-Longo

University of Torino, Department of Life Sciences and Systems Biology

Viale Mattioli 25, 10125, Torino, Italy

Tel. +39-011-6705972 // Fax +39-011-6705962

sergio.favero@unito.it

Abstract

Hyphal penetration, mineral dissolution and neoformation at the lichen-rock interface have been widely characterized by microscopic and spectroscopic studies, and considered as proxies of lichen deterioration of stone substrates. However, these phenomena have not been clearly related to experimental data on physical properties related to stone durability, and the physical consequences of lichen removal from stone surfaces have been also overlooked. In this study, we combine microscopic and spectroscopic characterization of the ~~interface between~~ structural organization of epi- and endolithic lichens (*Caloplaca marina* (Wedd.) Du Rietz, *Caloplaca ochracea* (Schaer.) Flagey, *Bagliettoa baldensis* (A.Massal.) Vězda, *Porina linearis* (Leight.) Zahlbr., *Verrucaria nigrescens* Pers.) ~~and at~~ the interface with limestones of interest for Cultural Heritage (Portland Limestone, Botticino Limestone), with analysis of rock properties (water absorption, surface hardness) relevant for durability, before and after the removal or scraping of lichen thalli. Observations using reflected-light and electron microscopy, and Raman analyses, showed lichen-limestone stratified interfaces, differing in the presence/absence and depth of lichen anatomical layers (lithocortex, photobiont layer, pervasive and sparse hyphal penetration component) depending on species and lithology. Specific structural organizations of lichen-rock interface were found to be associated with differential patterns of water absorption increase, evaluated by Karsten tube, in comparison with surfaces with microbial biofilms only, even more pronounced after the removal or scraping of the upper structural layers. Equotip measurements on surfaces bearing intact thalli showed lower hardness in comparison with control surfaces. By contrast, after the removal or scraping procedures, Equotip values were similar or higher than those of controls, suggesting that the increasing open porosity may be related to a biogenic hardening process. Such counterposed patterns of porosity increase and hardening need to be considered when models relating lichen occurrence on limestones and biogeomorphological surface evolution are proposed,

and to evaluate the ~~opportunity~~ consequences of lichen removal from stone-built cultural heritage.

Keywords

biodeterioration, lichen-rock interface, stone cultural heritage, surface hardness, water absorption capacity

Running head

Impact of lichens on limestone physical properties

Introduction:

Lithobiontic microorganisms are involved in multiple processes affecting rock surfaces at the atmosphere-lithosphere boundary [and the analogous surfaces of stones in buildings and structures](#) (Gorbushina and Broughton, 2009). Microbial influence on geomorphic processes is increasingly considered at all scales of landscape dynamics (e.g. Viles *et al.*, 2012; McIlroy de la Rosa, 2016). Colonization of modern and historic stonework is investigated for its implication for heritage conservation, with potential effects ranging from biodeterioration to bioprotection (Carter and Viles, 2005; Scheerer *et al.*, 2009; Kip and Van Veen, 2015; Tiano, 2016).

A [pedogenetic-weathering](#) role of lichens ~~has been long recognized~~, as pioneer colonizers of natural rock surfaces, [has been long recognized](#) (Jones, 1988). Lichen deterioration of stone in cultural heritage has also been widely characterized (reviewed, e.g., by St. Clair and Seaward, 2004; Gazzano *et al.*, 2009; Seaward, 2015), although evidence of protective effects has been also unveiled (e.g. McIlroy de la Rosa *et al.*, 2012, 2014, with references therein). Biogeophysical and biogeochemical processes at the rock surface have been ascribed to the attachment and penetration of epilithic and endolithic lichens, and their release of primary and secondary metabolites with acidic and chelating functions, respectively (Adamo and Violante, 2000; Chen *et al.*, 2000; Favero-Longo *et al.*, 2011; Salvadori and Casanova-Municchia, 2016). Advances in microscopic techniques have progressively supported a deeper characterization of lichen structures and associated microbes at the rock interface and their spatial interactions with microstructural features of the substrate and its mineral constituents (de los Ríos and Ascaso, 2005; Favero-Longo *et al.*, 2005; McIlroy de la Rosa *et al.*, 2012; Casanova-Municchia *et al.*, 2014; Mihajlovski *et al.*, 2015). Advanced spectroscopies have allowed the localization and characterization of chemical changes in minerals affected by lichen metabolites (Wierzchos and Ascaso, 1994; Barker and Banfield, 1996) and the detection at the interface of secondary minerals,

including clays and biomineralization products (Wierzchos and Ascaso, 1998; Edwards *et al.*, 2003; Villar *et al.*, 2004). However, such phenomena, considered as proxies to ascertain and quantify ~~the~~ rock weathering, have rarely been experimentally related to the durability of stone surfaces and their physical properties.

The influence of lichens on the hardness of rock surfaces has been evaluated for silicate lithologies colonized by epilithic and chasmoendolithic species (i.e. inhabiting cracks and fissures; sensu Golubic *et al.*, 1981) ~~through~~ across different climatic areas (McCarroll and Viles, 1995; Matthews and Owen, 2008; Guglielmin *et al.*, 2012; Favero-Longo *et al.*, 2015), but poorly explored for calcareous rocks. Some lichen species have been shown to variously affect the thermal response and moisture retention of limestones, potentially influencing their susceptibility to breakdown (Carter and Viles, 2003, 2004). A waterproofing influence of lichen colonization on the capillary coefficient of oolitic limestones has also been described (Concha-Lozano *et al.*, 2012). However, these studies only partially characterized the lichen component and its physico-chemical interaction with the substrate.

This study combines the characterization of lichen physico-chemical interactions with limestones of cultural heritage interest with the analysis of surface properties relevant for stone durability and weathering. We aimed to verify if the presence of ~~epilithic and euendolithic (i.e. actively penetrating; sensu Golubic *et al.*, 1981)~~ lichens, before and after their removal from the rock surface, may influence/modify the hardness and water absorption characteristics of Portland and Botticino limestones —in comparison with exposed surfaces colonized by microbial biofilms only (which are used in this study to represent surfaces exposed to abiotic and biotic weathering, but not colonized by lichens), or freshly broken surfaces (which are used in this study to represent uncolonized unweathered surfaces—in this study). In particular, we aimed to examine if the specific structural organization of some epilithic and euendolithic (i.e. actively penetrating; sensu

Golubic *et al.*, 1981) lichens at the rock interface may be related to different effects on limestone physical properties and potential weathering dynamics in natural environments and on stone-built cultural heritage. The structural organization of the lichen-rock interface was microscopically (reflected light and scanning electron microscopy) and spectroscopically (Raman) characterized, examining the hyphal penetration component (sensu Favero-Longo *et al.*, 2005) for epilithic species and the lithocortex, photobiont and pseudomedulla (sensu Pinna *et al.*, 1998) layers for endolithic species. Surface hardness and absorption capacity/infiltration rates were quantified by Equotip and Karsten tube, respectively.

Materials and methods

Lithologies and lichens

Two limestones largely employed in historical and modern building were sampled in abandoned quarry areas in the Isle of Portland in Dorset (SW-England; WGS-84: N 50°32.334' - W 2°25.548') and Botticino (N-Italy; WGS-84: N 45°32.965' - E 10°18.946'). The samples of Portland Limestone (P), collected in a maritime environment, were representative of a pure-calcite oolitic limestone (Brunsden *et al.*, 1996; Dubelaar *et al.*, 2003). Those of Botticino Limestone (B), deriving from a prealpine area, were micritic, low-magnesium calcite limestones (Borghi *et al.*, 2015). For each lithology, blocks (l × w × h: 15-30 × 15-20 × 15-20 cm) colonized by (a) microbial biofilms—(as controls exposed to abiotic and biotic weathering, but not colonized by lichens), (b) epilithic and (c) endolithic lichens were selected for investigations (Figure 1). Biofilms on P and B were composed of filamentous and coccoid green algae, with subordinate cyanobacteria (P-a), and microcolonial fungi and coccoid cyanobacteria (B-a), respectively. Epilithic crustose lichens included *Caloplaca* species with a discontinuous thallus [*Caloplaca marina* (Wedd.) Du Rietz on P: P-bC; *Caloplaca ochracea* (Schaer.) Flagey on B: B-bC], and, on B only,

Verrucaria nigrescens Pers. (B-bV) with a continuous thallus. Endolithic lichens included *Bagliettoa baldensis* (A.Massal.) Vězda (P-cB and B-cB) and, on P only, *Porina linearis* (Leight.) Zahlbr. (P-cP). Nomenclature follows Smith *et al.* (2009). Freshly broken surfaces of the blocks were also considered as controls, representative of unweathered surfaces (d).

Four and five blocks were investigated for P and B, respectively (Figure 1), according to availability in the sampling sites of suitable blocks which hosted all the different colonization types. On each block, measuring areas were established for each colonization type (one surface of approx. 3 cm² for biofilm and freshly broken controls; one mature thallus for each species of epilithic and endolithic lichens). On each measuring area, measures were sequentially performed on: (i) surface hardness and (ii) water absorption capacity. Measures on areas colonized by lichens were repeated one day after the thalli were removed, as described below, to simulate the decay of senescent/dead thalli on natural outcrops and their cleaning on monumental surfaces. Additional measuring areas on each block were also established for each colonization type to characterize the lichen-rock interface by (iii) reflected light (RLM) and scanning electron (SEM) microscopy, and (iv) Raman spectroscopy.

The removal of the lichen thalli from the rock surfaces was carried out, after ~~wetted-wetting~~ the measuring areas, under a stereomicroscope ~~to avoid causing any mechanical damage~~. For epilithic lichens, the thalline areaolae (TC, sensu Favero-Longo *et al.*, 2005) were gently removed using a scalpel, leaving ~~intact~~ the medulla-rock interface intact. Endolithic lichen thalli were also gently scraped with a scalpel until the algal layer was exposed, substantially removing their lithocortex (sensu Pinna *et al.*, 1998). Repeated observations of representative cross-sectioned materials, before and after the removal of epilithic and endolithic thalli, confirmed that the defined procedures avoided causing mechanical damages detectable by RLM.

Reflected light and scanning electron microscopy

The growth of microbial biofilms on and/or below the rock surface, and the lichen-rock interface were examined under reflected light (RLM) and scanning electron (SEM) microscopy.

RLM observations were carried out by an Olympus SZH10 on cross sections (approx. 2-5 × 5-10 × 0.5 cm h × l × w, at least 3 sections per colonization type per block) cut with a diamond saw and stained using the periodic acid - Schiff (PAS) to visualize the biological component within the lithic substrate (Favero-Longo *et al.*, 2005). The profile of the lichen-rock interface ([i.e. the structural organization of epilithic and endolithic lichens at the rock interface](#)) was characterized by measuring thickness and depths of morphologically/physiognomically different layers at randomly selected vertical transects.

SEM observations were carried out by a Scanning Electron Microscope JEOL JSM IT300LV (High Vacuum - Low Vacuum 10/650 Pa - 0.3-30kV) on carbon-coated analogous cross sections and fracture samples to morphologically evaluate the hyphal-mineral interactions at the different layers of the lichen-rock interface. Images acquired in back-scattered (BSE) modes (BED-C and BED-S) were also acquired, on representative cross-sections for the different colonization types, to visualize the ratio between granules (light grey-coloured in BSE) and voids including grain boundaries, pores and cracks (porosity sensu lato, s.l., black coloured in BSE) in fresh parts of the lithotypes and at the lichen interface (Sardini *et al.*, 2006; Favero-Longo *et al.*, 2009). Images were processed by a pixel-based colour classification using the software ImageJ 1.50i (National Institutes of Health, Bethesda, Maryland, USA). Cross sections and fracture samples are conserved in the Lichen-Petrographic Collection of the Herbarium of the University of Torino (Gazzano *et al.*, 2007).

Raman spectroscopy

Raman spectra were collected at the different layers of the lichen-rock interface with a micro-spectrometer Horiba Jobin-Yvon HR800 equipped with an HeNe laser at an excitation wavelength of 632.8 nm, a CCD air-cooled detector operating at -70°C, and an Olympus BX41 light microscope. The spectra were compared with those contained in the Raman Spectra Database of Minerals and Inorganics and in Bernstein *et al.* (2002), Edwards *et al.* (2003) and Casanova-Municchia *et al.* (2014).

Karsten tube

A Karsten tube, a small open-ended glass vial, was attached to the rock face using a sealant compound based on plastic (Plastic-Fermit white; Fermit: Vettelschoß, Germany) to measure water [absorption capacity penetration](#) (Mol and Viles, 2012). By measuring the decrease in water level (Δ) in the tube over a period of four hours, the water absorption per square centimetre [of rock surface](#) was calculated. Measurements were taken every 5 minutes for the duration of the 240 minutes' infiltration time and recorded as ml/7.065 mm² min (infiltration surface of the Karsten tube, manufacturer's specifications). For each measuring area (i.e. colonization type x block, before and after removal procedures), measurements were replicated five times, each measure being performed after the absence of residual moisture had been verified with a CEM-dt 128 Pinless Moisture Meter (Shenzhen Everbest Machinery Industry Co., China) and, in any case, at least after one day. The three most consistent absorption curves were used for calculating average values of

$$(\Delta t_n - \Delta t_0)/A \text{ (eq. 2)}$$

at $t_n = 15 \text{ min } (t_1), 30 \text{ min } (t_2), 60 \text{ min } (t_3), 120 \text{ min } (t_4) \text{ and } 240 \text{ min } (t_5)$, with $t_0 = 0 \text{ min}$.

Average values of

($\Delta_{t+10min} - \Delta_t$)/A (eq. 3)

were also calculated for t = 5→230 min, and used to calculate the average absorption rate for each ten minutes interval between the different time points (t_n and t_{n+1}).

Differences among the overall colonization types and between-types differences were tested applying non-parametric statistics Kruskal-Wallis and Mann-Whitney U Test, respectively, using Systat 10.2 (SYSTAT, Evanston, IL, USA). The data were visualized as boxplots obtained using RStudio (version 0.99.489 - © 2009-2015 RStudio, Inc.).

Equotip

Variability in block surface hardness was measured using a Proceq Equotip Piccolo 2, DL-type (Proceq, [USA/Switzerland](#)), a rock surface hardness rebound device ideal for use on soft and weathered surfaces (Viles *et al.*, 2011; Wilhelm *et al.*, 2016a). In the Equotip Piccolo 2, a 2.78 mm diameter spherical tungsten carbide test tip is mounted in an impact body and impacts at 11.1 N mm under spring force against the test surface from which it rebounds. The DL probe (tungsten carbide, 2.78 mm) was used as it is able to obtain readings in confined spaces [and thus suited the sometimes rough surfaces](#). The velocity before impact (V_1) and after impact (V_2) are measured automatically and displayed as a ratio ($V_2/V_1 \times 1000$) which is denoted by the Leeb Hardness (HL) unit (measuring range: 250-970 HLDL [using the DL probe](#)).

For each measuring area (colonization type x block), a combination of two measuring procedures [single impact method (SIM) and repeated impact method (RIM)] was adopted to provide a more robust ~~data~~-evaluation [of surface hardness characteristics](#) (Yilmaz, 2013; Wilhelm *et al.*, 2016b). A series of [45](#) randomly distributed ~~45~~-readings (SIM; for a confidence level of 95%) was firstly carried out to evaluate the elastic and plastic properties of the rock surfaces covered by the different colonization types. A second series

of 20 repeated measurements (RIM) on five points was then taken to characterize the elastic and plastic properties of the surface and subsurface of the colonized rock, reflecting strength characteristics such as the consolidation of mineral grains, the looseness of the original rock surface, and the degree of compaction due to repeated impacts (Aoki and Matsukura, 2007). After the removal of lichen thalli, a third series of randomly distributed readings (SIM) and a fourth one of repeated measurements (RIM) were analogously carried out to evaluate the rock hardness below/after the removal or scraping of the thalline component and lithocortex for epilithic and endolithic lichens, respectively.

The median value of the SIM series ($HLDL_{S.med}$) and the median of the maximum values of the five RIM series ($HLDL_{R.med}$) were used to calculate for each measuring area the robust hybrid dynamic hardness (HDH_{robust} , sensu Wilhelm *et al.*, 2016b) as follows:

$$HDH_{robust} = (HLDL_{S.med})^2 / (HLDL_{R.med}) \text{ (eq. 1)}$$

Differences among the overall colonization types and between-types differences were tested applying non-parametric statistics Kruskal-Wallis and Mann-Whitney U Test, respectively, using Systat 10.2 (SYSTAT, Evanston, IL, USA). The data were visualized as boxplots obtained using RStudio (version 0.99.489 - © 2009-2015 RStudio, Inc.).

Results

Microscopy and Raman spectroscopy at the lichen-rock interface

RLM observations on cross sections showed for all epilithic and endolithic lichen species a stratified interface with the underlying substrate, developed from the surface [within into](#) the interior of Portland (Figure 2) and Botticino (Figure 3) limestones. By contrast, the investigated microbial biofilms mostly grew epilithically on the calcareous surfaces, poor penetration of associated hyphal structures being only sporadically observed (Figures 2a-b, 3a-b).

The following lichen-rock interface layers were recognized, which were present or absent depending on the species and on the colonized lithology (Table 1): lithocortex (LI, sensu Pinna *et al.*, 1998), endolithic photobiont layer (PL, sensu Pinna *et al.*, 1998), pervasive (pHPC) and sparse (sHPC) hyphal penetration component (sensu Favero-Longo *et al.*, 2005, equivalent for endolithic species to the pseudomedulla layer, sensu Pinna *et al.*, 1998). The lichen-rock interface organization mostly varied among species with regard to the presence/absence of LI and PL layers and on the thickness and depths of pHPC and sHPC layers (Table 1; additional photographic profiles of the lichen-rock interface in Supplementary material 1). Each species generally showed a similar organization on the two lithotypes with regard to LI, PL and pHPC layers, while sHPC layer was generally negligible in Botticino.

In particular, cross sections showed that *Caloplaca marina* and *C. ochracea* (Figures 2c-d, 3c-d) discontinuously developed a 100-300 µm thick epilithic thalline component (sensu Favero-Longo *et al.*, 2005), including photobionts, or a 100-200 µm thick endolithic PL (sensu Pinna *et al.*, 1998) immersed beneath a crystalline film. Beneath these upper “alternative” layers, both the lithotypes were penetrated by an approx. 100-300 µm thick pHPC, followed by a sHPC down to a depth of approx. 1.0 mm. Beneath its truly epilithic

thalli, *Verrucaria nigrescens* (Figures 3e-f) developed a thicker pHPC (approx. 600-800 μm), while a deeper sHPC was poorly observed.

Both *Bagliettoa baldensis* (Figures 2g-h, 3g-h) and *Porina linearis* (Figures 2e-f) developed truly endolithic thalli with a 70-150 μm thick immersed PL, but remarkably differed for the presence of a prominent 50-100 μm thick LI (sensu Pinna *et al.*, 1998) in the former species (Figure 4a). Beneath the PL, the pHPC of *Bagliettoa baldensis* penetrated the Portland and Botticino limestones down to depths of approx. 300-700 μm and 150-400 μm , respectively. A sHPC was observed in Portland down to depths of approx. 2.0-3.0 mm, while it was scarce in Botticino. *Porina linearis* developed pHPC within the Portland limestone down to 300-1200 μm , while a deeper, sHPC was observed down to 2.0-3.0 mm. For all the species, diffuse PAS staining at the pHPC level likely indicated an abundance of extracellular polymeric substances (EPS), which were instead less detected at the other layers.

RLM observations on Portland revealed at the interface with the different species a loss of the oolitic appearance down to depths of approx. 100-500 μm , while a lower layer, down to 700-1000 μm , still showed its oolitic structure, but darker hues. At the lichen-Botticino interface some colour shift was observed down to 300-500 μm , but the rock microstructure was unmodified.

SEM observations highlighted at the different interface layers the hyphal organization and localization with respect to the mineral component, clarifying differences between the endolithic lichen species on Portland. BSE mode observations at the LI and PL of *B. baldensis* displayed a poor signal of the mineral component, indicating dominance of voids occupied by the biotic component (porosity s.l., observed by BSE imaging, over than 50%; Figure 4b). Conglutination of hyphae and microcrystals was another prominent feature at these layers (Figure 4c). Beneath LI and PL, a decreasing of voids at increasing distance from the surface was recognizable (porosity s.l. at the PL-LI >> pHPC >> sHPC >

1
2
3
4
5
6
7 uncolonized layer and freshly broken controls; Figure 4b and Supplementary material 2).
8
9 In *P. linearis*, photobionts were sparse in the early 150 µm beneath the surface (Figure
10 4d), where the oolitic structure was masked (Figures 4e-f). At the pHPC layer, penetrating
11 hyphae were strictly intermingled with microcrystals (Figures 4g-h). Beneath this layer,
12
13 hyphae were more sparsely observed, but densely occurred densely within wider rock
14
15 discontinuities (Figure 4i). A similar interface structure also characterized *C. marina* in
16
17 Portland. By contrast, in the case of *C. ochracea* and *B. baldensis* within Botticino, the
18
19 hyphal occurrence beneath the algal layer was mostly related with the local occurrence of
20
21 wide discontinuities (Figure 4l). BSE observations on lichen species on Botticino confirmed
22
23 the pervasive, but shallow HPC development beneath the surface, where the increase of
24
25 dark colours indicated a lichen-related increased porosity down to 600-800 µm in depth
26
27 (e.g. porosity s.l., observed by BSE imaging, at the pHPC of *V. nigrescens* >> uncolonized
28
29 layer > freshly broken controls; Figure 4m and Supplementary material 2).
30
31 Raman spectroscopy at the lichen-rock interface of all the endolithic and epilithic species
32
33 consistently displayed spectra attributable to calcite, while oxalates were never detected.
34
35 At the LI and PL layers of endolithic species, spectral bands with wavenumber at 1520 and
36
37 1161 cm⁻¹, assignable to C=C and C-C stretching modes, respectively, and likely
38
39 attributable to carotenoids (Bernstein *et al.*, 2002; Casanova-Municchia *et al.*, 2014) were
40
41 also observed, while only the calcite vibrational modes were detected at the deeper layers
42
43 and in the bulk (Supplementary material 3).
44
45

46 *Water absorption capacity*

47
48 Karsten tube measurements showed different absorption capacities of limestone surfaces
49
50 affected by the different colonization types, and a general increase of absorption capacity
51
52 of surfaces colonized by lichens after the removal and scraping of epilithic and endolithic
53
54 thalli, respectively (Figure 5; Supplementary material 4).
55
56
57
58
59
60

On both lithologies and for all the colonization types, higher absorption rates were detected at the t_0 - t_1 and t_1 - t_2 intervals, while values (and variability) progressively decreased and became stable at the successive measuring intervals. Different colonization types, however, displayed different effects on the absorption patterns. On Portland (Figure 5), both rate and cumulative values showed significantly higher absorption for surfaces colonized by *B. baldensis*, before and after the scraping, and *P. linearis* after the scraping, with respect to those colonized by microbial biofilms and *Porina linearis* before the scraping. Surfaces colonized by *C. marina* also showed low values, but thalli on the examined blocks did not allow enough measurements to be collected to run statistical analyses. On Botticino (Supplementary material 4), surfaces colonized by *B. baldensis*, before and after the scraping, and *C. ochracea* and *V. nigrescens*, after thallus removal, showed higher absolute values of water absorption, but also in this case only a limited set of reliable data was collected because deep internal cracks often compromised measures, preventing any statistical analyses.

Hybrid dynamic hardness

Equotip measurements showed that some of the epilithic and endolithic lichens affected the hardness of the Portland and Botticino surfaces when compared to controls. Although a high spread of values was detected for some study cases, the hybrid dynamic hardness ($\text{HDH}_{\text{robust}}$; Figure 6) and the hardness measured by single impact method (HLDL_S) (Supplementary material 6) of surfaces colonized by lichens was generally lower than that of exposed surfaces with microbial biofilms only and of freshly broken ones. Whereas in contrast, higher $\text{HDH}_{\text{robust}}$ and HLDL_S values characterized the same surfaces after the removal of thalline component and scraping of lithocortex for epilithic and endolithic species, respectively. Hardness measured by repeated impact method (HLDL_R) was rather steady before and after removal and scraping procedures (Supplementary material 6).

Portland surfaces colonized by *B. baldensis* showed, in particular, significantly lower HDH_{robust} and $HLDL_S$ values than all the other colonization types. On Botticino, the lowest average values were obtained when Equotip was applied on the thick and thin epilithic thalli of *V. nigrescens* and *C. ochracea*, respectively, while surfaces colonized by *B. baldensis* displayed HDH_{robust} and $HLDL_S$ values slightly lower than those with epilithic biofilms.

After the scraping or removal procedures, Portland and Botticino surfaces differed in the fact that the former generally showed HDH_{robust} and $HLDL_S$ values higher than those of controls (freshly broken surfaces and surfaces with microbial biofilms only), while the latter showed values similar to those of controls.

Discussion

By combining the microscopical characterization of lichen-limestone interface with direct measures of water absorption capacity and hardness, this study illustrates how lichen colonization of the surface and interior of limestones affects physical properties potentially relevant for durability. Specific structural organizations of epilithic and endolithic lichens on/within the rocks were associated to differential patterns of water absorption increase with respect to surfaces with microbial biofilms, even more pronounced after the removal or scraping of their upper structural layers (thalline component and lithocortex for epilithic and endolithic species, respectively). Increased water absorption was likely related to the absorption behaviour of intact thalli and the within-rock discontinuities penetrated by hyphae, more exposed after the removal or scraping procedures. However, measures by Equotip, informative on elastic and plastic properties of stone surfaces and subsurfaces, and proxy of open porosity (Wilhelm *et al.*, 2016b), revealed another related scenario. Only surfaces bearing intact thalli showed lower values of hybrid dynamic hardness (HDH_{robust}), related to compressibility, and hardness measured by single impact method ($HLDL_S$) with

respect to control surfaces, freshly broken or colonized by microbial biofilms. By contrast, after the removal or scraping procedures, the HDH_{robust} and HLDL_S values were similar or higher than those of controls, suggesting that a biogenic hardening process may accompany the increasing open porosity ~~may be related to a biogenic hardening process~~. In the following sub-sections, we discuss the recognized structural layers of epilithic and endolithic lichen-limestone interface (*Structural organization of the lichen-rock interface*) to support the understanding of correlations between lichen colonization and limestone physical properties (*Lichen influence on the physical properties of limestones and weathering*).

Structural organization of the lichen-rock interface

Microscopic investigations exhibited have found differential layered arrangements of the lichen-rock interface within a wide set of lithologies (de los Ríos and Ascaso, 2005; Favero-Longo *et al.*, 2005; Casanova-Municchia *et al.*, 2014). Specific structural layers observed for the examined epilithic and endolithic lichens, recognized within both the Portland and Botticino limestones, were consistent with reports on several carbonate lithologies for the same species and/or others with similar functional traits and ecological requirements (Pinna *et al.*, 1998; Bungartz *et al.*, 2004; Hoppert *et al.*, 2004; Favero-Longo *et al.*, 2009; McIlroy de la Rosa *et al.*, 2012). In the endolithic *Bagliettoa baldensis* and *Porina linearis*, the development of fruiting bodies was remarkably associated with pitting phenomena, widely recognized as a prominent effect of endolithic lichens on carbonate rocks (Salvadori and Casanova Municchia, 2016). The thickness ranges of PL ~~were~~ ~~as~~ analogous to the dataset ~~of~~ ~~by~~ Pinna *et al.* (1998), as related to the light harvesting capacity. Microscopy and Raman analyses displayed for *B. baldensis* an upper lithocortex, composed of fine-grained calcite surrounding sparse hyphae. Such a layer, less prominent in *P. linearis*, morphologically resembled the fine-grained micrite layer described for the

1
2
3
4
5
6
7
8
9
10
11
12
13
14
15
16
17
18
19
20
21
22
23
24
25
26
27
28
29
30
31
32
33
34
35
36
37
38
39
40
41
42
43
44
45
46
47
48
49
50
51
52
53
54
55
56
57
58
59
60

endolithic *Verrucaria rubrocincta* on [caliche](#) limestone (Bungartz *et al.*, 2004), and recognized as a biomineralization product by isotope analyses (Garvie *et al.*, 2008). Depths of pHPC, ranging from few hundreds of microns to approx. 1 mm, differed between species (Pinna *et al.*, 1998), but were also more related to the two lithotypes. Higher total porosity of Portland limestone, confirmed for the sample set with SEM-BSE observations, likely favoured a more extensive development of pHPC and the occurrence of a sHPC down to depths of 2-4 mm, which was scarce in the less porous Botticino. Differences in type and extent of porosity s.l. [were have](#) indeed [been](#) recognized as relevant factors to determine the extent of fungal colonization within sedimentary rocks (Cámara *et al.*, 2008). On the other hand, the rock volume penetrated by the sHPC displayed an increase of porosity s.l. (secondary porosity) with respect to the deeper layers, according to the active dissolution processes related to the growth of endolithic lichens (Salvadori and Casanova-Municchia, 2016). In Portland, this pattern was related to a pronounced hyphal intragranular penetration and the loss of the oolitic appearance, also observed in other oolitic limestones penetrated by Verrucariaceae (Concha-Lozano *et al.*, 2012). Presence of oxalates, debated with regard to the endolithic lichen-rock interface (Bungartz *et al.*, 2004), was not observed here, according to previous findings of Pinna *et al.* (1998). The areolate thalline component of *Verrucaria nigrescens*, displaying a truly epilithic structure, was associated with a thick pHPC down [to](#) 800 µm, compatible to the range of depths reported for the same species in other carbonate lithologies (Favero-Longo *et al.*, 2009). The *Verrucaria* pHPC layer displayed higher porosity with respect to uncolonized deeper layers, suggesting lichen related dissolution processes (Cámara *et al.*, 2008; Favero-Longo *et al.*, 2009). Although *Caloplaca ochracea* has been reported as epilithic (Smith *et al.*, 2009), anatomical observation of the cross-sectioned discontinuous thalli confirmed previously recognized difficulties in classifying its growth form (Pinna *et al.*, 1998) and reports as

endolithic species (Nimis and Martellos, 2008). Our observations disclosed similar issues for *C. marina*. As the thalline component (TC) was discontinuously present, wide parts of the thalli were immersed within the limestones, showing a layered structure similar to the truly endolithic *B. baldensis* (LI-PL-HPC).

Lichen influence on the physical properties of limestones and weathering

The data collected with Karsten tube and Equotip on lichen-covered, microbial biofilm-covered and freshly broken surfaces allow directly comparable observations of the physical properties of limestones with and without lichen cover. Lichen colonization has been proposed to contribute to the development of micro- and meso-scale weathering morphologies and to affect the overall rate of karstification (Mc Ilroy de la Rosa et al., 2012; Mc Ilroy de la Rosa 2016). The suggested models, also supposing the potential succession of different communities during the long and complex surface histories, considered the lichen effect on a timescale which is not compatible with direct observations (McIlroy de la Rosa et al., 2012; Viles, 2012). In this work, influences of lichen colonization on the physical properties of Portland and Botticino limestones were considered during the presence of living thalli on/within the rocks and immediately after the removal or scraping of their upper structural layers, simulating their natural decay or cleaning work by restorers.

In some cases (in particular for Botticino), the rock blocks selected for analyses finally revealed a restricted availability of surfaces colonized by lichens suitable to run the time-consuming Karsten-tube measures (5 measures of 4 hours per sample replicate with operator's check-times of 5 min), limiting the collection of a dataset suitable for statistical analyses. Nevertheless, our findings offer a first experimentally-supported insight on the influence of epilithic and endolithic lichens on the water absorption capacity of limestones and their hardness response to single and repeated impacts.

1
2
3
4
5
6
7
8
9
10
11
12
13
14
15
16
17
18
19
20
21
22
23
24
25
26
27
28
29
30
31
32
33
34
35
36
37
38
39
40
41
42
43
44
45
46
47
48
49
50
51
52
53
54
55
56
57
58
59
60

On both Portland and Botticino, our analyses showed the highest water absorption values ~~for on~~ surfaces colonized by the LI-bearing *Bagliettoa* ~~highest values of absorption~~, while those of epilithic species, *Porina linearis* (without a prominent LI-layer), and the microbial biofilms were rather similar. Epilithic lichens, in particular *Verrucaria nigrescens*, have been shown to retain moisture on limestone (Saint Quentin) surfaces (Carter and Viles, 2003) and ~~were have been~~ suggested to play an umbrella-like protection with respect to deteriorogenic endolithic species, as *Bagliettoa baldensis* (Carter and Viles, 2005). By contrast, occurrence of *Bagliettoa baldensis* on Burren limestone ~~was has been~~ shown to reduce dissolution processes if compared to bare surfaces (McIlroy de la Rosa *et al.*, 2014). Similarly, a surface-sealing effect of the lithocortex of *Verrucaria rubrocincta*, anatomically similar to the LI of examined species, has also been hypothesized on Sonoran caliche limestone (Bungartz *et al.*, 2004). ~~With this regard, o~~Our observations showed an increase in water absorption after the removal/scraping procedures, which likely removed the sealing effect and made accessible the primary porosities and the secondary ones related to pHPC, shown by SEM-BSE observations. ~~Accordingly, a~~ similar loss of water-proofing effect of endolithic Verrucariaceae on oolitic limestones ~~has~~ been reported after sandblasting and calcification of surfaces, but poorly related to the lichen structural features (Concha-Lozano *et al.*, 2012).

Combination of single and repeated impact measures with Equotip showed lower HLDL_s and HDH_{robust} values for surfaces bearing intact thalli ~~lower HLDL_s and HDH_{robust} values~~ than freshly broken and microbial colonized controls. These values were respectively related to hardness and compressibility of the biological (thalline component) or biomineralized (lithocortex) layers with respect to the mineral ones, on which they have a cushion-like effect. Similarly results have been found in Antarctica where, hardness measures on lichens gave lower values than bare surfaces when carried out directly on epilithic thalli (Guglielmin *et al.*, 2012). After the removal and scraping of upper layers, and

the exposure of secondary porosity, as revealed by Karsten tube, $HLDL_S$ and HDH_{robust} values were similar (Botticino) or even higher (Portland) than those of controls. Although the rock layers occupied by pHPC displayed higher porosity and exhibited a mineral-leached structure, their elastic and plastic properties appeared improved with respect to freshly broken and microbial biofilm controls. Such findings support the recent hypothesis that lichens were responsible for higher hardness ($HLDL_S$) of uncleaned Portland headstones with respect to regularly cleaned ones (Wilhelm *et al.*, 2016b). As biogenic calcite of several biological systems, as seashells, was shown to display superior hardness, and model synthetic calcite crystals with contents of amino acids revealed enhanced hardness (Kim *et al.*, 2016), our results suggest the opportunity to investigate if and how hardening patterns may also deal with accompany lichen biogeochemical processes on limestones.

Our observations have implications for the contribution of lichens to weathering of limestone in natural and cultural settings, as well as for the impacts of removing lichens from stone in cultural heritage. Lichen colonization has been proposed to contribute to the development of micro- and meso-scale weathering morphologies and to affect the overall rate of karstification (McIlroy de la Rosa *et al.*, 2012; McIlroy de la Rosa 2016). The suggested models, also supposing the potential succession of different communities during the long and complex surface histories, considered the lichen effect on a timescale which is not compatible with direct observations (McIlroy de la Rosa *et al.*, 2013; Viles, 2012). In this work, influences of lichen colonization on the physical properties of Portland and Botticino limestones were considered during the presence of living thalli on/within the rocks and immediately after the removal or scraping of their upper structural layers, simulating their natural decay or cleaning work by restorers, and can thus contribute to evaluating and refining geomorphological models of lichen biomodification.

Formatted: Italian (Italy)

Formatted: English (U.K.)

Mcllroy de la Rosa *et al.* (2013) propose two models illustrating the short-term bioprotective role of lichens (with and without calcium oxalate encrustation) followed by episodic accelerated weathering when the thalline shielding and calcium oxalate encrustation effects are removed following death of the lichen. The findings in this study provide support for this sort of temporal sequence (through comparison of lichen-covered with freshly-broken surfaces), but reveal the importance of lichen-induced biogenic hardening in the absence of calcium oxalate precipitation as an additional factor not considered by Mcllroy de la Rosa *et al.* (2013). Comparisons between microbial biofilm-covered, freshly-broken and lichen-covered surfaces can also throw light on the third and fourth models of Mcllroy de la Rosa *et al.* (2013), which address longer term evolution of karstic surfaces where dynamic relations between lichen biomodifications and dissolution processes are predicted. The findings in this study help refine and calibrate such models. Truly bare surfaces, with only abiotic dissolution, are highly unlikely in most natural karst environments and thus using biofilm-covered surfaces as a control improves the model. Furthermore, findings such as harder surface characteristics and lower water penetration rates on microbial biofilm-covered surfaces indicating lower weathering rates than those produced by the net effect of lichen growth and decay (lichen-covered and freshly broken surfaces) in Portland and Botticino.

Concluding remarks
Conclusions

Lichens have variously been claimed to be biodeteriorative or bioprotective on rocks depending on lithologies and several other factors (Seaward, 2015; Salvadori and Casanova Municchia, 2016). On limestone, the hyphal penetration and surface biomineralization by endolithic *Verrucaria rubrocincta* has even been explained as simultaneous counter-balancing processes yielding deterioration and protection, respectively (Bungartz *et al.*, 2004). Our work was not limited to consider lichen

development within rocks and biomineralization phenomena as proxies of deterioration or protection, but ~~first characterized lichen-rock interaction by relating~~ also related detailed observations of lichen-rock interactions with ~~these patterns with~~ physical properties of limestone potentially relevant to durability and weathering, i.e. water penetration and surface hardness. Limestone substrate colonized by epilithic and endolithic lichen structures generally displayed an increased water absorption capacity due to lichen-induced secondary porosity, generally associated with increased stone decay (Karaca, 2010). By contrast, the lichen-rock interface revealed unmodified or even increased hardness of limestone, often related to higher durability (and lower weathering rates) of many different lithologies (Guglielmin *et al.*, 2012; Mol and Viles, 2012). Although such counterposed patterns should be still verified on a wider range of limestone lithologies in different (micro-)climate conditions, these findings need to be taken into account when models relating lichen occurrence on limestones and biogeomorphological surface evolution are proposed (McIlroy de la Rosa *et al.*, 2012, 2013). Our analyses, indeed, confirmed the working hypothesis that limestones colonized by lichens display physical properties, such as hardness and water absorption, which are different from surfaces exposed to other abiotic and biotic weathering factors, likely influencing their morphological evolution. Moreover, the documented biogeomorphological significance of lichens appears diverse depending on the structural organization at the rock interface of the different epilithic and endolithic species. In general, however, deterioration related to hyphal penetration in limestone is likely counterbalanced by a parallel protective effect of lichens, which lasts while the rock surface is covered by thalline component and lithocortex of epilithic and endolithic species, respectively, which provide an umbrella-like effect and limit erosion processes. Subsequent decay/removal of the upper structural layers of lichens expose surfaces with higher permeability, but hardened, likely prone to flaking, as

described for case-hardened siliceous surfaces (Dorn, 2013). The stability of natural limestone surfaces may be thus in part related to the persistence of lichen communities. Future research should verify whether and, if so, which other weathering processes may follow the potential decay of the hyphal penetration component and the ecological succession of other microbial lithobionts in the endolithic microniche previously occupied by lichens. Environmental variations related to global change dynamics potentially affecting lichen communities and their decay rate may indirectly affect the geomorphological dynamics, even before being directly effective on them (see Viles and Cutler, 2012). In particular, differential effects on limestone physical properties recorded for different epilithic and endolithic species imply that equilibria between lichen communities and biogeomorphological dynamics may be mediated by the selective responses of each species to environmental pressures. Furthermore, the fact that limestone surfaces colonized by lichens become a biogeomaterial with peculiar physical properties, modified with respect to the fresh stone, should be considered when policies of conservation or removal of lichen cover from the stone cultural heritage have to be established.

Acknowledgements

MM is a recipient of a doctoral fellowship funded by INPS (Istituto Nazionale di Previdenza Sociale, Italy). The authors are grateful to the Editor in Chief, Prof. Stuart N. Lane, and two anonymous reviewers for helpful and constructive comments, ~~are grateful~~ to Consorzio Produttori Marmo Botticino Classico for access~~ion~~ to the quarry area and to Mona Edwards and Hong Zhang (Oxford Rock Breakdown Laboratory, University of Oxford) for technical assistance. MM particularly thanks Vanessa Winchester (University of Oxford) for precious discussions on British lichens.

References

- Adamo P, Violante P. 2000. Weathering of rocks and neogenesis of minerals associated with lichen activity. *Applied Clay Science* **16**: 229-256.
- [Aoki H, Matsukura Y. 2007. A new technique for non-destructive field measurement of rock-surface strength: an application of the Equotip hardness tester to weathering studies. *Earth Surface Processes and Landforms* **32**: 1759-1769.](#)
- Barker WW, Banfield JF. 1996. Biologically versus inorganically mediated weathering reactions: relationships between minerals and extracellular microbial polymers in lithobiontic communities. *Chemical Geology* **132**: 55-69.
- Bernstein PS, Zhao DY, Wintch SW, Ermakov IV, McClane RW, Gellermann W. 2002. Resonance Raman measurement of macular carotenoids in normal subjects and in age-related macular degeneration patients. *Ophthalmology* **109**: 1780-1787.
- Borghi A, Berra V, d'Atri A, Dino GA, Gallo LM, Giacobino E, Martire L, Massato G, Vaggelli G, Bertok C, Castelli D, Costa E, Ferrando S, Groppo C, Rolfo F. 2015. Stone materials used for monumental buildings in the historical centre of Turin (NW Italy): Architectonical survey and petrographic Characterization of Via Roma. *Geological Society, London, Special Publications* **407**: 201–18.
- Brunsden D, Coombe K, Goudie AS, Parker AG. 1996. The structural geomorphology of the Isle of Portland, southern England. *Proceedings of the Geologists' Association*, **107**: 209-230.
- Bungartz F, Garvie LAJ. 2004. Anatomy of the endolithic Sonoran Desert lichen *Verrucaria rubrocincta* Breuss: implications for biodeterioration and biomineralization. *Lichenologist* **36**: 55-73.
- Cámara B., De los Ríos A, García del Cura MA, Galván V, Ascaso C. 2008. Dolostone bioreceptivity to fungal colonization. *Materiales de Construcción* **58**: 113-124.

Carter NEA, Viles HA. 2005. Bioprotection explored: the story of a little known earth surface process. *Geomorphology* **67**: 273-81.

Carter NEA, Viles HA. 2004. Lichen hotspots: raised rock temperatures beneath *Verrucaria nigrescens* on limestone. *Geomorphology* **62**: 1-16.

Carter NEA, Viles HA. 2003. Experimental investigations into the interactions between moisture, rock surface temperatures and an epilithic lichen cover in the bioprotection of limestone. *Building and Environment* **38**: 1225-34.

Casanova Municchia AG, Caneva G, Ricci MA, Sodo A. 2014. Identification of endolithic traces on stone monuments and natural outcrops: preliminary evidences. *Journal of Raman Spectroscopy* **45**: 1180-1185.

Chen J, Blume H-P, Beyer L. 2000. Weathering of rocks induced by lichen colonization-a review». *Catena* **39**: 121-146.

Concha-Lozano N, Gaudon P, Pages J, de Billerbeck G, Lafon D, Eterradosi O. 2012. Protective effect of endolithic fungal hyphae on oolitic limestone buildings. *Journal of Cultural Heritage* **13**: 120-27.

De los Rios A, Ascaso C. 2005. Contributions of in situ microscopy to the current understanding of stone biodeterioration. *International Microbiology* **8**: 181-188.

[Dorn RI. 2013. Rock coatings. In Treatise on Geomorphology, vol. 4, Weathering and Soils Geomorphology, Shroder J, Pope GA \(eds\). Academic Press: San Diego \(USA\); 70-97.](#)

Dubelaar CW, Engering S, Van Hees RPJ, Koch R, Lorenz HG. 2003. Lithofacies and petrophysical properties of Portland Base Bed and Portland Whit Bed limestone as related to durability. *Heron* **48**: 221-229.

Edwards HG, Seaward MR, Attwood SJ, Little SJ, de Oliveira LF, Tretiach M. 2003. FT-Raman spectroscopy of lichens on dolomitic rocks: an assessment of metal oxalate formation. *Analyst* **128**: 1218-1221.

- Favero-Longo SE, Accattino E, Matteucci E, Borghi A, Piervittori R. 2015. Weakening of gneiss surfaces colonized by endolithic lichens in the temperate climate area of northwest Italy. *Earth Surface Processes and Landforms* **40**: 2000-2012.
- Favero-Longo SE, Gazzano C, Girlanda M, Castelli D, Tretiach M, Baiocchi C, Piervittori R. 2011. Physical and chemical deterioration of silicate and carbonate rocks by meristematic microcolonial fungi and endolithic lichens (Chaetothyriomycetidae). *Geomicrobiology Journal* **28**: 732-744.
- Favero-Longo SE, Borghi A, Tretiach M, Piervittori R. 2009. In vitro receptivity of carbonate rocks to endolithic lichen-forming aposymbionts. *Mycological research* **113**: 1216-1227.
- Favero-Longo SE, Castelli D, Salvadori O, Belluso E, Piervittori R. 2005. Pedogenetic action of the lichens *Lecidea atrobrunnea*, *Rhizocarpon geographicum* gr. and *Sporastatia testudinea* on serpentinized ultramafic rocks in an alpine environment. *International Biodeterioration & Biodegradation* **56**: 17-27.
- Garvie LA, Knauth LP, Bungartz F, Klonowski S, Nash III TH. 2008. Life in extreme environments: survival strategy of the endolithic desert lichen *Verrucaria rubrocincta*. *Naturwissenschaften* **95**: 705-712.
- Gazzano C, Favero-Longo SE, Matteucci E, Roccardi A, Piervittori R. 2009. Index of Lichen Potential Biodeteriogenic Activity (LPBA): a tentative tool to evaluate the lichen impact on stonework. *International Biodeterioration & Biodegradation* **63**: 836-843.
- Gazzano C, Favero-Longo SE, Matteucci E, Castelli D, Piervittori R. 2007. Allestimento di una collezione licheno-petrografica presso l'Erbario Crittogamico di Torino per lo studio del biodeterioramento di rocce e materiali lapidei. In *Lo stato dell'arte 5: V Congresso nazionale IGIIIC: Cremona, 11-13 ottobre 2007*. Nardini: Firenze; 669-677.
- Golubic S, Friedmann I, Schneider J. 1981. The lithobiontic ecological niche, with special reference to microorganisms. *Journal of Sedimentary Research* **51**: 475-478.

Gorbushina AA, Broughton WJ. 2009. Microbiology of the atmosphere-rock interface: how biological interactions and physical stresses modulate a sophisticated microbial ecosystem. *Annual Review of Microbiology* **63**: 431–450.

Guglielmin M, Worland MR, Convey P, Cannone N. 2012. Schmidt Hammer studies in the Maritime Antarctic: application to dating Holocene deglaciation and estimating the effects of macrolichens on rock weathering. *Geomorphology* **155–56**: 34–44.

Hoppert M, Flies C, Pohl W, Günzl B, Schneider J. 2004. Colonization strategies of lithobiontic microorganisms on carbonate rocks. *Environmental Geology* **46**: 421–428.

Jones D. 1988. Lichens and pedogenesis. In *Handbook of lichenology, Volume 3*, Galun M (ed). CRC Press: Boca Raton (USA); 109–124.

Karaca Z. 2010. Water absorption and dehydration of natural stones versus time. *Construction and Building Materials* **24**: 786–790.

Kim YY, Carloni JD, Demarchi B, Sparks D, Reid DG, Kunitake ME, Tang CC, DUER MJ, Freeman CL, Pokroy B, Penkman K, Harding JH, Estro LA, Baker SP, Meldrum FC. 2016. Tuning hardness in calcite by incorporation of amino acids. *Nature materials* **15**: 903–910.

Kip N, van Veen JA. 2015. The dual role of microbes in corrosion. *The ISME Journal* **9**: 542–551.

Matthews JA, Owen G. 2008. Endolithic lichens, rapid biological weathering and Schmidt hammer r-values on recently exposed rock surfaces: Storbreen glacier foreland, Jotunheimen, Norway». *Geografiska Annaler: Series A, Physical Geography* **90**: 287–97.

McCarroll D, Viles H. 1995. Rock-weathering by the lichen *Lecidea auriculata* in an arctic alpine environment. *Earth Surface Processes and Landforms* **20**: 199–206.

- Mcllroy de la Rosa, JP. 2016. The Burren: a glacial, karstic and biokarstic expression of a limestone plateau in western Ireland. *Earth Surface Processes and Landforms* 41: 1614-1628.
- Mcllroy de la Rosa, JP, Warke PA, Smith BJ. 2012. Microscale biopitting by the endolithic lichen *Verrucaria baldensis* and its proposed role in mesoscale solution basin development on limestone: the role of *Verrucaria baldensis* in solution basin development". *Earth Surface Processes and Landforms* 37: 374-384.
- Mcllroy de la Rosa JPM, Warke PA, Smith BJ. 2013. Lichen-induced biomodification of calcareous surfaces: bioprotection versus biodeterioration. *Progress in Physical Geography* 37: 325-351.
- Mcllroy de la Rosa JP, Warke PA, Smith BJ. 2014. The effects of lichen cover upon the rate of solutional weathering of limestone. *Geomorphology* 220: 81-92.
- Mihajlovski A, Seyer D, Benamara H, Bousta F, Di Martino P. 2015. An overview of techniques for the characterization and quantification of microbial colonization on stone monuments. *Annals of Microbiology* 65: 1243-1255.
- Mol L, Viles HA. 2012. The role of rock surface hardness and internal moisture in tafoni development in sandstone: internal moisture and tafoni development in sandstone. *Earth Surface Processes and Landforms* 37: 301-314.
- Nimis PL, Martellos S. 2008: *ITALIC - The Information System on Italian Lichens*. Version 4.0. University of Trieste, Dept. of Biology, IN4.0/1 (<http://dbiodbs.univ.trieste.it/>). Accessed on 15th September 2016.
- Pinna D, Salvadori O, Tretiach M. 1998. "An anatomical investigation of calcicolous endolithic lichens from the Trieste Karst (NE Italy). *Plant Biosystems* 132: 183-195.
- Salvadori O, Casanova Municchia A. 2016. The Role of Fungi and Lichens in the Biodeterioration of Stone Monuments. *The Open Conference Proceedings Journal* 7: 39-54.

Sardini P, Siitari-Kauppi M, Beaufort D, Hellmuth KH. 2006. On the connected porosity of mineral aggregates in crystalline rocks. *American Mineralogist* **91**: 1068-1080.

Scheerer S, Ortega-Morales O, Gaylarde C. 2009. Microbial deterioration of stone monuments - An updated overview. *Advances in Applied Microbiology* **66**: 97-139.

Seaward MRD. 2015. Lichens as agents of biodeterioration. In *Recent Advances in Lichenology, Volume 1*, Upreti DA, Divakar PK, Shukla V, Bajpai (eds). Springer India: New Dehli; 189-211.

Smith CW. 2009. *Lichens of Great Britain and Ireland*. British Lichen Society: London.

St. Clair LL, Seaward MRD. *Biodeterioration of stone surfaces. Lichens and biofilms as weathering agents of rocks and cultural heritage*. Kluwer Academic Publishers, Dordrecht.

Tiano P. 2016. Biodeterioration of stone monuments: a worldwide Issue». *The Open Conference Proceedings Journal* **7**: 29-38.

Viles HA. 2012. Microbial geomorphology: a neglected link between life and landscape. *Geomorphology* **157-158**: 6-16.

Viles HA, Cutler NA. 2012. Global environmental change and the biology of heritage structures. *Global Change Biology*, **18**: 2406-2418.

Viles H, Goudie A, Grab S, Lalley J. 2011. The use of the Schmidt Hammer and Equotip for rock hardness assessment in geomorphology and heritage science: a comparative analysis. *Earth Surface Processes and Landforms* **36**: 320-33.

Villar SE, Edwards HGM, Seaward MRD. 2004. Lichen biodeterioration of ecclesiastical monuments in Northern Spain. *Spectrochimica Acta Part A: Molecular and Biomolecular Spectroscopy* **60**: 1229-37.

Wierzbos J, Ascaso C. 1994. Application of back-scattered electron imaging to the study of the lichen-rock interface. *Journal of Microscopy* **175**: 54-59.

- Wierzchos J, Ascaso C. 1998. Mineralogical transformation of bioweathered granitic biotite, studied by HRTEM: evidence for a new pathway in lichen activity. *Clays and Clay Minerals* **46**: 446-452.
- Wilhelm K, Viles H, Burke O. 2016a. Low impact surface hardness testing (Equotip) on porous surfaces - advances in methodology with implications for rock weathering and stone deterioration research: Equotip hardness testing on porous rock and stone». *Earth Surface Processes and Landforms* **41**: 1009-1152.
- Wilhelm K, Viles H, Burke O, Mayaud J. 2016b. Surface hardness as a proxy for weathering behaviour of limestone heritage: a case study on dated headstones on the Isle of Portland, UK. *Environmental Earth Sciences* **75**, 1-16.
- Yilmaz NG. 2013. The influence of testing procedures on uniaxial compressive strength prediction of carbonate rocks from Equotip Hardness Tester (EHT) and proposal of a new testing methodology: hybrid dynamic hardness (HDH). *Rock Mechanics and Rock Engineering* **46**: 95-106.

Figure captions

Figure 1. Lithobiont colonization types examined on Portland (P) and Botticino (B) limestones. Measurements of water absorption capacity and hardness were carried out by Karsten tube and Equotip on block surfaces, while the thickness and depth of the thalline (TC) and hyphal penetration (HPC) components (sensu Favero-Longo *et al.*, 2005) of epilithic and endolithic lichens were examined on cross-sectioned profiles. Study cases are schematically summarized on the right picture side: (a) epilithic microbial biofilm on Portland (P-a) and Botticino (B-a); (b) epilithic lichens on Portland, *Caloplaca marina* (P-bC), and on Botticino, *Caloplaca ochracea* (B-bC) and *Verrucaria nigrescens* (B-bV); (c) endolithic lichens on Portland, *Porina linearis* (P-cP) and *Bagliettoa baldensis* (P-cB), and on Botticino, *Bagliettoa baldensis* (B-cB); d-freshly broken surfaces of Portland (P-d) and Botticino (B-d).

Figure 2. Lithobiont growth within the Portland limestone (cross sections observed under RLM before –a,c,d,g- and after – b,d,f,h – staining by PAS): (a, b) epilithic microbial biofilm; (c, d) *Caloplaca marina*; (e, f) *Porina linearis*; (g, h) *Bagliettoa baldensis*. Reproductive structures (RS), the photobiont layers (PL) and lithocortex (LI) of lichens are recognizable before the staining step, which highlights the development of the hyphal penetration component (pHPC = pervasive hyphal penetration component; sHPC = sparse hyphal penetration component) beneath the rock surface (dotted white line). Microbial biofilm (MB). Sparse hyphae (SH) were sporadically observed beneath the epilithic biofilm. Scales: black bar. Further lithobiont profiles are reported in Supplementary material 1.

Figure 3. Lithobiont growth within the Botticino limestone (cross sections observed under RLM before –a,c,d,g- and after – b,d,f,h – staining by PAS): (a, b) epilithic microbial biofilm; (c, d) *Caloplaca ochracea*; (e, f) *Verrucaria nigrescens*; (g, h) *Bagliettoa baldensis*. Reproductive structures (RS), the photobiont layers (PL) and lithocortex (LI) of lichens are

recognizable before the staining step, which highlights the development of the hyphal penetration component (pHPC = pervasive hyphal penetration component; sHPC = sparse hyphal penetration component) beneath the rock surface (dotted white line). Microbial biofilm (MB). Sparse hyphae (SH) were sporadically observed beneath the epilithic biofilm. Scales: black bar. Further lithobiont profiles are reported in Supplementary material 1.

Figure 4. Anatomy of the lichen-rock interface as observed by RLM (a, d). Scales: black bar. and SEM in secondary electron (c, f, g, i, l) and BSE (BED-C: h, m; BED-S: b, e) modes (Scales: white bar). *Bagliettoa baldensis* (a-c) and *Porina linearis* (d-i) within Portland: (a, d) lithocortex and photobiont layers (LI-PL); (b) lichen-rock interface profile; (c) microcrystals at the lithocortex layer (LI), reproductive structures (RS); (e-f) appearance of the oolytic structure (OO) at the photobiont and deeper layers; (g-h) hyphae intermingled with microcrystals at the pHPC layers, associated to secondary porosity; (i) hyphae (H) within rock discontinuities at the sHPC layer; (l) *Bagliettoa baldensis* within Botticino: hyphae within rock discontinuities; (m) *Verrucaria nigrescens*-Botticino interface profile.

Figure 5. Water absorption capacity of Portland limestone colonized by microbial biofilm (P-a), epilithic (P-bC: *Caloplaca marina*) and endolithic (P-cP: *Porina linearis*; P-cB: *Bagliettoa baldensis*) lichens, before (white boxes) and after (grey boxes) removal/scraping procedures. Average absorption rate for each ten minutes interval between the different time points (left column) and total absorption at the different time points (right column). Time-points: 15 min (t_1), 30 min (t_2), 60 min (t_3), 120 min (t_4) and 240 min (t_5), with $t_0 = 0$ min. Boxes which do not share at least one letter are statistically different (Kruskal-Wallis and Mann-Whitney U Test; $p \leq 0.05$). Overview tables of statistical analyses are reported in Supplementary material 5.

Figure 6. Hybrid dynamic hardness (HDH_{robust}) of (P) Portland limestone, freshly broken (P-d), colonized by microbial biofilm (P-a), epilithic (P-bC: *Caloplaca marina*) and endolithic (P-cB: *Bagliettoa baldensis*; P-cP: *Porina linearis*) lichens, before (white boxes) and after (grey boxes) removal/scraping procedures, and (B) Botticino limestone, freshly broken (B-d), colonized by microbial biofilm (B-a), epilithic (B-bC: *Caloplaca ochracea*; B-bV: *Verrucaria nigrescens*) and endolithic (B-cB: *Bagliettoa baldensis*) lichens, before (white boxes) and after (grey boxes, REM) removal/scraping procedures. Boxes which do not share at least one letter are statistically different (Kruskal-Wallis and Mann-Whitney U Test; $p \leq 0.05$). Overview tables of statistical analyses are reported in Supplementary material 7.